Inorganic Chemistry

Article

pubs.acs.org/IC

Picolyl−NHC Hydrotris(pyrazolyl)borate Ruthenium(II) Complexes: Synthesis, Characterization, and Reactivity with Small Molecules

Francys E. Fernández, M. Carmen Puerta,* and Pedro Valerga*

Departamento de Ciencia de los Materiales e Ingeniería Metalúrgica y Química Inorgánica, Facultad de Ciencias, Universidad de Cádiz, 11510 Puerto Real, Cádiz, España

Supporting Information

ABSTRACT: Ruthenium(II) hydrotris(pyrazolyl)borate chloro complexes bearing picolyl-functionalized N-heterocyclic carbenes [TpRu(κ^2-*C,N*-**picolyl-^{R}I**)Cl] (picolyl-^{Me}I = 3-methyl-1-(2-picolyl)imidazol-2-ylidene) (**1a**), picolyl-^{iPr}I = 3-isopropyl-1-(2-picolyl)imidazol-2-ylidene (**1b**), picolyl-^{Me}45DClI = 3-methyl-1-(2-picolyl)-4,5-dichloroimidazol-2-ylidene (**1c**), picolyl-^{Ph}I = 3-phenyl-1-(2-picolyl)imidazol-2-ylidene (**1d**), picolyl-^{Me}BI = 3-methyl-1-(2-picolyl)benzoimidazol-2-ylidene (**1e**)) have been synthesized and characterized. Furthermore, cationic carbonyl derivatives **2a−e** have been prepared, characterized, and used to study the donor properties of the picolylcarbene ligands (**picolyl-^{R}I**) via infrared spectroscopy. Also, the reactivity of the 16-electron species [TpRu(κ^2-*C,N*-**picolyl-^{R}I**)]$^+$, in situ generated using $NaBAr^F_4$ (Ar^F = 3,5-bis(trifluoromethyl)phenyl) as a halide scavenger, toward N_2, CH_3CN, H_2, CH_2CH_2, S_8, and O_2 was studied indicating a strong influence of the NHC wingtip and backbone substituents in the product distribution. The crystal structures of [TpRu(κ^2-*C,N*-picolyl-^{iPr}I)Cl] (**1b**), [TpRu(κ^2-*C,N*-picolyl-^{Me}I)CO][BAr^F_4] (**2a**), [TpRu(κ^2-*C,N*-picolyl-^{Ph}I)CO][BAr^F_4] (**2d**), [{TpRu(κ^2-*C,N*-picolyl-^{Me}I}$_2$(μ-N_2)][BAr^F_4]$_2$ (**3′a**), [{TpRu(κ^2-*C,N*-picolyl-^{Ph}I)}$_2$(μ-N_2)][BAr^F_4]$_2$ (**3′d**), [TpRu(κ^2-*C,N*-picolyl-^{iPr}I)(η^2-CH_2CH_2)][BAr^F_4] (**5b**), and [{TpRu(κ^2-*C,N*-picolyl-^{Me}I)}$_2$(μ-S_2)][BAr^F_4]$_2$ (**6**) are reported.

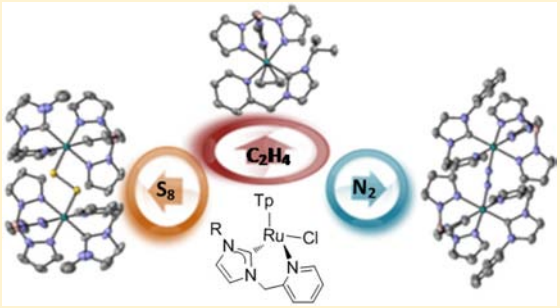

INTRODUCTION

Bidentate N-heterocyclic carbene (NHC) based ligands have been widely used in organometallic chemistry for the synthesis of homogeneous catalysts.[1] The potential hemilability of the new donor group, capable of reversible dissociation from the metal center,[2] has led to the synthesis of NHCs functionalized with phosphine,[3] pyrimidine,[4] ether,[5] thioether,[6] carboxylate,[7] indenyl,[8] oxazoline,[9] and pyridine.[10] Ligands with nitrogen donors have attracted most attention; particularly, metal complexes bearing pyridine functionalized NHCs of Ir,[11] Ag,[12] Pd,[13] Ru,[14] and Ni[15] have been synthesized. Among nitrogen donors, picoline has been used to generate *N*-picolyl-NHC ligands, which can be easily synthesized with different substitution patterns on the picoline ring and the NHC.[16] This leads to a versatile ligand group toward the study of coordination properties.

Since its introduction by Trofimenko in 1966, the hydrotris(pyrazolyl)borate (Tp) ligand has been extensively used as a spectator ligand in transition metal chemistry because it binds strongly to metals and is resistant toward electrophilic and nucleophilic attacks.[17] Tp is generally compared with C_5R_5 due to the fact that both of them donate the same number of electrons (6 electrons) and adopt a facial geometry generating typically half-sandwich complexes. However, there are noteworthy differences between the two ligand classes.[18] The cone angle of Tp is close to 180° well above the 100° and 146° estimated for C_5H_5 and C_5Me_5, respectively. Thus the steric bulk of Tp disfavors higher coordination numbers of the metal center. Also, Tp ligand has lower field strength compared with C_5R_5 ligands, with its nitrogen atoms acting as σ donors, while C_5R_5 group is capable of π donation. Besides, the [TpRu]$^+$ preferentially adopts a six-coordinated structure, in contrast with C_5R_5 analogues that are capable of forming seven-coordinated species. Ruthenium compounds with cyclopentadienyl type ligands have been broadly studied because they are able to give rise to metastable 16-electron species with many potential catalytic applications.[19] Particularly, half-sandwich ruthenium complexes bearing monodentate NHCs have proven to be active in olefin metathesis,[20] racemization of chiral alcohols,[21] alkyne dimerization,[22] and isomerization of allylic alcohols.[23] Also, our group has recently synthesized a series of [(η^5-C_5Me_5)Ru(κ^2-*C,N*-picolyl-NHCs)CH_3CN][PF_6] complexes and studied the influence of N-heterocyclic carbene ligands in catalytic transfer hydrogenation of ketones and imines.[24] However, ruthenium hydrotris(pyrazolyl)borate complexes bearing NHCs are rare; to the best of our knowledge, only two examples of Tp−ruthenium complexes bearing a monodentate NHC have been reported. In 2001, Grubbs and co-workers published the synthesis of [(κ^3-Tp)($IMesH_2$)(Cl)-Ru=CHPh] shown in Figure 1a upon studying the reactivity of a ruthenium benzylidene complex, ($IMesH_2$)-

Received: November 21, 2012
Published: March 26, 2013

   dx.doi.org/10.1021/ic302553z | *Inorg. Chem.* 2013, 52, 4396−4410

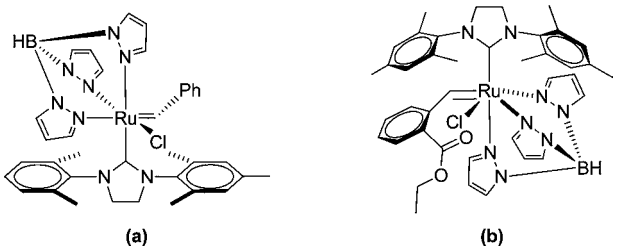

Figure 1. (a) $[(\kappa^3\text{-Tp})(\text{IMesH}_2)(\text{Cl})\text{Ru}{=}\text{CHPh}]$[25] and (b) $[(\kappa^3\text{-Tp})\text{Ru}(\text{IMesH}_2)(\text{Cl})\text{Ru}{=}\text{CH}(2\text{-COOEtPh})]$.[26]

$(\text{Cl})_2(\text{C}_5\text{H}_5\text{N}_2)_2\text{Ru}{=}\text{CHPh}$.[25] In addition, Burtscher et al. reported the synthesis of $[(\kappa^3\text{-Tp})\text{Ru}(\text{IMesH}_2)(\text{Cl})\text{Ru}{=}\text{CH}(2\text{-COOEtPh})]$ presented in Figure 1b while studying the reactivity of (SPY-5-34)-dichloro(κ^2-(C,O)-2-ethoxycarbonylbezylidene)(H_2IMes)ruthenium (SPY = square pyramidal; 5 = coordination number; 34 = diastereoisomer index).[26] Thus, Tp−ruthenium complexes containing functionalized N-heterocyclic carbene ligands have not been reported, and they represent a new ruthenium scaffold for the exploration of reactivity and its application on several catalytic processes.

Our group has broad experience with the stoichiometric chemistry of hydrotris(pyrazolyl)borate ruthenium complexes bearing PR_3, P,P, and P,N ligands.[27] We aim to replace the phosphine fragment by an NHC to study the effect of the new ligands in the reactivity of the metal center. In this work, we describe a series of novel hydrotris(pyrazolyl)borate ruthenium-(II) picolyl-NHC complexes in which the ligands have been varied systematically. In addition, small molecule activation is an area of interest, considering its significant impact in several biological, industrial, and environmental processes. The in situ generation of the 16-electron fragment, $[\text{TpRu}(\kappa^2\text{-}C,N\text{-picolyl-NHC})]^+$, using a halide scavenger, NaBAr^F_4 (Ar^F = 3,5-bis(trifluoromethyl)phenyl), allowed us to study the reactivity of the new ruthenium compounds toward small molecules, such as CO, N_2, CH_3CN, H_2, CH_2CH_2, S_8, and O_2. The crystal structures of $[\text{TpRu}(\kappa^2\text{-}C,N\text{-picolyl-}^{i\text{Pr}}\text{I})\text{Cl}]$ (**1b**), $[\text{TpRu}(\kappa^2\text{-}C,N\text{-picolyl-}^{\text{Me}}\text{I})\text{CO}][\text{BAr}^\text{F}_4]$ (**2a**), $[\text{TpRu}(\kappa^2\text{-}C,N\text{-picolyl-}^{\text{Ph}}\text{I})\text{CO}][\text{BAr}^\text{F}_4]$ (**2d**), $[\{\text{TpRu}(\kappa^2\text{-}C,N\text{-picolyl-}^{\text{Me}}\text{I})\}_2(\mu\text{-N}_2)][\text{BAr}^\text{F}_4]_2$ (**3′a**), $[\{\text{TpRu}(\kappa^2\text{-}C,N\text{-picolyl-}^{\text{Ph}}\text{I})\}_2(\mu\text{-N}_2)][\text{BAr}^\text{F}_4]_2$ (**3′d**), $[\text{TpRu}(\kappa^2\text{-}C,N\text{-picolyl-}^{i\text{Pr}}\text{I})(\eta^2\text{-CH}_2\text{CH}_2)][\text{BAr}^\text{F}_4]$ (**5b**), and $[\{\text{TpRu}(\kappa^2\text{-}C,N\text{-picolyl-}^{\text{Me}}\text{I})\}_2(\mu\text{-S}_2)][\text{BAr}^\text{F}_4]_2$ (**6**) have been determined, in order to contribute to the scarce crystallographic library of Tp−ruthenium NHC complexes. After a judicious literature search, it is remarkable that here we report the first example of structural characterization of a TpRu disulfide complex $[\text{Tp}(\kappa^2\text{-}C,N\text{-picolyl-}^{\text{Me}}\text{I})\text{Ru}{-}\text{S}{-}\text{S}{-}\text{RuTp}(\kappa^2\text{-}C,N\text{-picolyl-}^{\text{Me}}\text{I})]^{2+}$, **6**, along with the first TpRu dinitrogen bridged complexes bearing an NHC $[\text{Tp}(\kappa^2\text{-}C,N\text{-picolyl-}^{R}\text{I})\text{Ru}{-}\text{N}{\equiv}\text{N}{-}\text{Ru}(\kappa^2\text{-}C,N\text{-picolyl-}^{R}\text{I})\text{Tp}]^{2+}$, **3′a** and **3′d**, and the first TpRu ethylene complex, $[\text{TpRu}(\kappa^2\text{-}C,N\text{-picolyl-}^{i\text{Pr}}\text{I})(\text{CH}_2\text{CH}_2)]^+$, **5b**. There is only one additional example of structural characterization of a TpRu dinitrogen bridged complex containing PCy_3 as a ligand.[28]

RESULTS AND DISCUSSION

Synthesis of κ^3-Hydrotris(pyrazolyl)borate Picolyl-NHC Ru(II) Complexes. The Ru(II) neutral complexes **1a**−**e** (Scheme 1) have been prepared upon treatment of the metal precursor [TpRu(COD)Cl] with a solution of the appropriate silver carbene, previously generated via reaction of silver oxide and picolyl imidazolium salts, **a**-**e**, in 1,2-dichloroethane.

Scheme 1

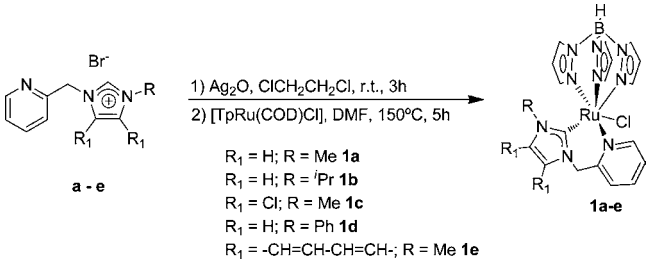

Initially, the synthetic route of choice was the in situ generation of the free carbene by treatment of the picolyl imidazolium salts with a strong base (i.e., Li^{n}Bu or KO^{t}Bu) in THF, followed by the addition of the metal precursor. However, a mixture of products and starting material, as evidenced in the ^{1}H NMR spectra of the reaction mixture, was obtained in all cases. $\text{TpRu}(\text{PPh}_3)_2\text{Cl}$ was also used as an alternative metal precursor, but the presence of coordinated phosphine in the generated products was evident in every attempt, in addition to an uncharacterizable mixture of complexes. Hence, the transmetalation method was the route of choice to afford the new Ru(II) complexes **1a**−**e**, given that we had previously synthesized $[(\eta^6\text{-}p\text{-cymene})\text{Ru}^\text{II}(\text{picolyl-NHC})\text{Cl}][\text{PF}_6]$ using this method.[29] It is very important to note that after the metal precursor is added, the reaction mixture needs to be heated at high temperatures (150 °C) to complete the transmetalation process and that the desired products were not synthesized using a solvent other than DMF. Previously, Kirchner and co-workers have demonstrated that the COD ligand in the [TpRu(COD)Cl] precursor is substitutionably inert; only prolonged heating and high temperatures in boiling DMF led to $[\text{TpRu}(\text{L}_2)\text{Cl}]$ or $[\text{TpRu}(\text{L})_2\text{Cl}]$ (L = PPh_3, py, PCy_3, AsPh_3, CH_3CN; L_2 = tmeda, dppm, acac) products.[30] In our case, the silver picolyl-carbenes are stable under these conditions, and upon heating the reaction mixture for 5 h at 150 °C, **1a**−**e** were obtained in high yields (over 78%) in all cases. The new Ru(II) compounds were characterized by ^{1}H and $^{13}\text{C}\{^1\text{H}\}$ NMR and elemental analysis. All these ruthenium picolyl−NHC complexes are very soluble in THF, acetone, and chlorinated solvents but insoluble in other solvents such as hexane, Et_2O, and petroleum ether.

^{1}H NMR spectra of compounds **1a**−**e** lack the C_2 imidazolium proton resonance signals at 10−12 ppm, indicating the coordination of the C_2 carbene carbon to the metal center. Also, there are two characteristic AB doublet signals with coupling constants of 14−15 Hz corresponding to the methylene bridge protons, which become diastereotopic after coordination of the ligands to the Ru atom given the κ^2-C,N coordination. One of the methylene proton signals is particularly shifted to a lower field, up to 7.2 ppm, in comparison with other ruthenium picolyl−NHC complexes.[29,31] Similar NMR features on $(\eta^5\text{-}\text{C}_5\text{Me}_5)\text{Ru}$ and $(\eta^6\text{-}p\text{-cymene})\text{Ru}$ κ^2-P,N complexes bearing chelating phosphinopicoline or chelating κ^2-C,N pyridyl-NHC ligands have been observed.[29,31,32] Also, all nine nonequivalent characteristic Tp signals are observed in the ^{1}H NMR spectrum. The $^{13}\text{C}\{^1\text{H}\}$ NMR signals of the carbene carbons atoms of **1a**−**e** (192−211 ppm) are located as expected for Ru−NHC compounds.[19−24,29,31,32] It is interesting to note the displacement to lower field, up to 211 ppm, of the NMR resonance of the C_2 carbon atom corresponding to the benzoimidazol compound

dx.doi.org/10.1021/ic302553z | Inorg. Chem. 2013, 52, 4396−4410

1e. It is possible to explain this observation due to destabilization in the imidazolium ring conjugation produced by the attached benzene ring, which leads to a lower electron density in the C_2 carbon. In addition, this behavior was evidenced in the previous synthesis of the (η^5-C_5Me_5)Ru and (η^6-*p*-cymene)Ru picolyl-NHC analogues.[24,29,31]

Crystals of **1b** suitable for X-ray diffraction were obtained by slow diffusion of hexane in a dichloromethane solution. ORTEP diagram of the ruthenium(II) complex is displayed in Figure 2. From the mother liquor, a second set of **1b** crystals

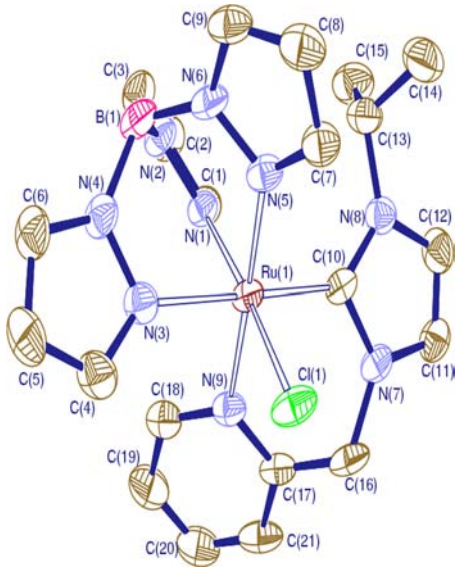

Figure 2. ORTEP diagram for complex **1b** [TpRuCl(κ^2-*C*,*N*-picolyl-^{iPr}I)] (picolyl-^{iPr}I = 3-isopropyl-1-(2-picolyl)imidazol-2-ylidene) with 50% probability ellipsoids. Hydrogen atoms have been omitted for clarity. Color code: Ru, red; N, blue; C, brown; B, pink; Cl, green.

was obtained, which showed residual silver bromide with the composition **1b**·0.35AgBr. Its structure has been determined by X-ray analysis (Figure S1 in Supporting Information).

As far as we know, no structure containing TpRu and a chelating NHC ligand has been previously described. The octahedral geometry of Ru in **1b** is distorted with the greatest deviation from linearity in the axis Cl(1)−Ru(1)−N(1), 172.86(9)°, and bond angles between ligands in cis, ranging from 84.35° to 95.23°. Imidazolyl and pyridyl rings form a dihedral angle of 52.24(23)°. These rings are almost aligned with the pyrazolyl rings trans to them, forming dihedral angles of 10.78(38)° for the imidazolyl ring and 14.10(38)° for the pyridyl ring, respectively. The bond lengths corresponding to Ru(1)−Cl(1), 2.4436(11) Å, and Ru(1)−C(10), 2.000(5) Å, are comparable with those reported for [TpRuClLL′] (L = 1,3-*bis*(2,4,6-trimethylphenyl)-4,5-dihydroimidazol-2-ylidene; L′ = 2-ethoxycarbonylbenzylidene).[26] They are also similar to those found for ruthenium *p*-cymene complexes containing 3-methyl-1-(2-picolyl)imidazol-2-ylidene) or 3-methyl-1-(2-picolyl)-4,5-dichloroimidazol-2-ylidene) ligands.[29] Ru−N bond lengths increase from 2.046(4) Å for N(1) trans to Cl(1) to 2.131(4) for N(3) trans to the imidazol-2-ylidene carbon C(10). This trans influence is also similar to that found for the above cited ruthenium complex [TpRuClLL′].[26]

The reactivity of the new ruthenium complexes toward small molecules was assessed upon in situ generation of the corresponding 16-electron species via reaction of **1a**−**e** with a halide scavenger, $NaBAr^F_4$ (Ar^F = 3,5-bis(trifluoromethyl)-phenyl), in fluorobenzene and in the presence of the appropriate substrate.

Reactivity of 1a−e with CO. A fluorobenzene solution of the appropriate TpRu(κ^2-*C*,*N*-picolyl-NHC)Cl precursor, **1a**−**e**, and $NaBAr^F_4$ was treated with 1 atm of CO. All complexes reacted irreversibly, generating the expected [TpRu(κ^2-*C*,*N*-picolyl-^{R}I)CO][BAr^F_4] complexes, **2a**−**e** (Scheme 2). The compounds were characterized by ^{1}H NMR, $^{13}C\{^1H\}$ NMR, elemental analysis, and IR.

Scheme 2

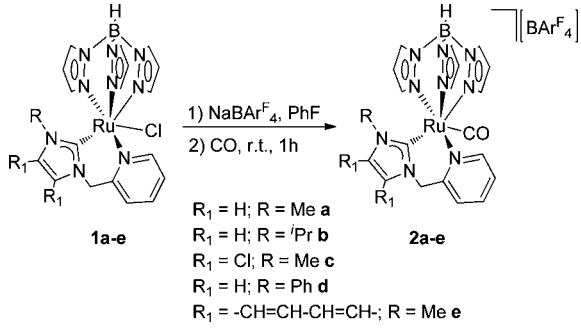

The data shown in Table 1 indicates that each compound displayed a single strong carbonyl absorption band between

Table 1. Selected IR (ν, cm^{-1}) and $^{13}C\{^1H\}$ NMR (δ, ppm) Data for Compounds 2a−e

		IR	$^{13}C\{^1H\}$	
entry	complex	ν(CO)	RuC≡O	C_2−NHC
1	**2a**	1964	203.0	177.5
2	**2b**	1973	203.2	175.2
3	**2c**	1984	204.0	180.4
4	**2d**	1976	204.6	177.0
5	**2e**	1976	205.9	168.6

1964 and 1984 cm^{-1}. In addition, important differences were observed between the donating properties of the picolyl−NHC ligands; particularly, **2c** showed a significantly higher value of stretching frequency (entry 3) in comparison with its analogue **2a** (entry 1). These results can be rationalized by the presence of the two chloro substituents in the imidazol backbone of **2c**, which led to a less donating imidazolydene ligand and a more electron deficient ruthenium center. Also, N-wingtip substituents have an influence in the donor properties of picolyl−NHC ligands, although less pronounced in comparison with the backbone substituents. Particularly, **2a** with a methyl group as wingtip showed the lowest CO stretching frequency (entry 1), while isopropyl and phenyl (entries 2 and 4) derivatives, **2b** and **2d**, showed higher stretching frequencies, indicating the stronger σ donating power of 3-methyl-1-(2-picolyl)-imidazolydene ligand in comparison with its analogues. Furthermore, the coordination of the carbonyl moiety led to a shift to high field of the C_2 carbene carbon resonance, as was predicted considering the weakening of the Ru−C_2 bond by the presence of a CO ligand. However, no significant differences are observed in the $^{13}C\{^1H\}$ NMR spectra of the carbonyl complexes, **2a**−**e**, regarding Ru−C_2 and RuCO $^{13}C\{^1H\}$ NMR chemical shifts.

dx.doi.org/10.1021/ic302553z | *Inorg. Chem.* 2013, 52, 4396−4410

Crystals of **2a** and **2d** suitable for X-ray diffraction were obtained after recrystallization from Et_2O/petroleum ether (1/2). ORTEP diagrams of [TpRu(κ^2-*C*,*N*-picolyl-^{Me}I)CO][BAr^F_4], **2a**, and [TpRu(κ^2-*C*,*N*-picolyl-^{Ph}I)CO][BAr^F_4], **2b**, are displayed in Figures 3 and 4, respectively.

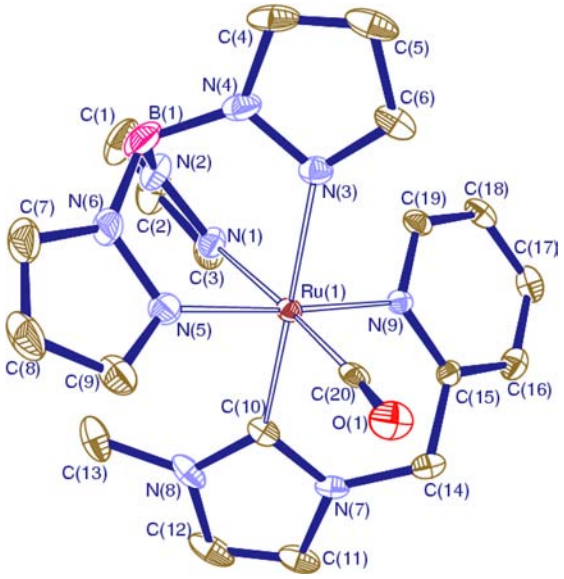

Figure 3. ORTEP diagram of the cation [TpRu(κ^2-*C*,*N*-picolyl-^{Me}I)(CO)]$^+$ (picolyl-^{Me}I = 3-methyl)1-(2-picolyl)imidazol-2-ylidene) in **2a** with 50% probability ellipsoids. Hydrogen atoms have been omitted for clarity. Color code: Ru, dark red; N, blue; C, brown; B, pink; O, red.

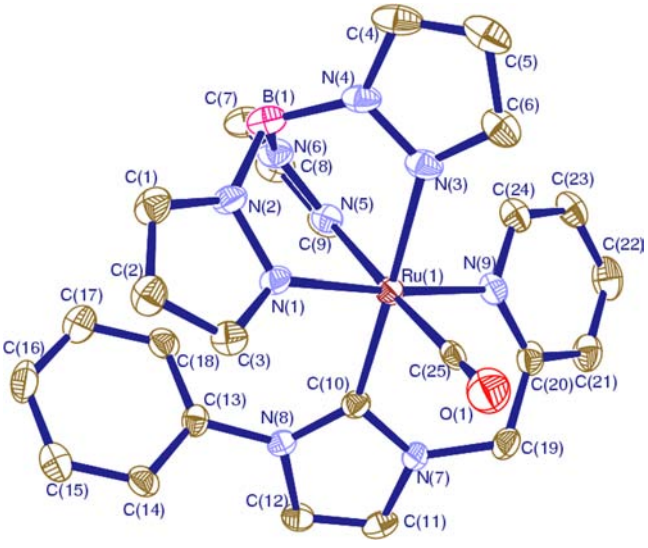

Figure 4. ORTEP diagram of the cation [TpRu(κ^2-*C*,*N*-picolyl-^{Ph}I)(CO)]$^+$ (picolyl-^{Ph}I = 3-phenyl-1-(2-picolyl)imidazol-2-ylidene) in **2d** with 50% probability ellipsoids. Hydrogen atoms have been omitted for clarity. Color code: Ru, dark red; N, blue; C, brown; B, pink; O, red.

As previously shown for the crystal structure of the neutral chlorocomplex, **1b**, the octahedron around Ru is distorted in cationic complexes [TpRu(κ^2-*C*,*N*-picolyl-^{Me}I)(CO)]$^+$, **2a**, and [TpRu(κ^2-*C*,*N*-picolyl-^{Ph}I)(CO)]$^+$, **2d**. The transverse axis to the C−Ru−C plane in **2a**, N(5)−Ru(1)−N(9) 174.34(11)°, and **2d**, N(1)−Ru(1)−N(9) 173.51(13), respectively, show the maximum deviation from linearity in each case. Bond angles between ligands in cis are in the range 85.22(13)−96.55(13)° for **2a** and 84.28(13)−95.48(14)° for **2d**. Imidazolyl and pyridyl rings in the chelating NHC ligand form a dihedral angle of 58.68(13)° for **2a** and 50.45(12)° for **2d**. These rings are more closely aligned with the pyrazolyl rings trans to them for **2a**, forming dihedral angles of 10.08(25)° for the imidazolyl ring and 10.22(28)° for the pyridyl ring, whereas for **2d**, the analogous dihedral angles are 20.52(0.19)° and 13.93(27)°, respectively. In both compounds, the shortest Ru−N bond length corresponds to the N atom of the pyrazolyl ring opposite to the pyridinic N atom, Ru(1)−N(5) 2.068(3)Å for **2a** and Ru(1)−N(1) 2.071(3)Å for **2d**. X-ray structures confirmed the IR data analysis conclusions, indicating a CO ligand more strongly bound to the metal in the case of the methyl derivative **2a**, Ru(1)−C(20) 1.866(4)Å than in the phenyl derivative **2d**, Ru(1)−C(25) 1.920(5) Å. Consequently, the π backbonding effect is larger in the first case showing a C−O bond length of 1.132(5) Å, which is in line with the mean value of 1.134(22) Å known for C≡O ligand bonded to Ru.[33]

Reactivity of 1a−e with N_2. A solution of the corresponding chloro complex, **1a−e**, in fluorobenzene under dinitrogen atmosphere was treated with a halide scavenger, $NaBAr^F_4$. The reactions afforded several nitrogen complexes. It is interesting to note that, upon reaction of **1a** and $NaBAr^F_4$ under 1 atm of nitrogen, two dinuclear dinitrogen bridged complexes, **3a** and **3′a**, were generated (Scheme 3). The dinitrogen complexes, **3a** and **3′a**, are diastereoisomers given the chiral character of the new ruthenium center in the bridged structure. The mixture of diastereoisomers was characterized by ^{1}H, ^{13}C{^{1}H}, and 2D ^{1}H,^{13}C NMR spectra, elemental analysis, IR, and Raman spectroscopy. Complexes **3a** and **3′a** were isolated as a mixture in a reproducible manner as the only species resulting from the reaction, in ca. 91% yield. The presence of two nonequivalent ruthenium centers is evidenced by the duplication of all proton and carbon signals in the NMR spectra corresponding to Tp and picolyl-^{Me}I ligands. However, both complexes are very similar in terms of chemical shifts, particularly the Ru−C_2−NHC carbon bonds in the ^{13}C{^{1}H} NMR spectrum appeared at 180.5 and 180.4 ppm, respectively. Also, it is very interesting that **3a** and **3′a** must be almost identical in stability because they are found as a 1/1 mixture, as evidenced by the ^{1}H NMR integrals.

Crystals of diastereomer **3′a** were obtained after recrystallization from Et_2O/petroleum ether (1/2). Although all the crystals evaluated proved to be racemic twinning, a structure was obtained by analysis as the twin of X-ray diffraction data in monoclinic space group *Pn*. ORTEP diagram of diastereomer **3′a** is displayed in Figure 5. To the best of our knowledge, **3′a** is the first TpRu nitrogen bridged complex synthesized using NHCs as ligands.

The structure of **3′a** shows the ruthenium atoms in a distorted octahedral geometry, with the largest deviation from linearity in the N−Ru−N≡N−Ru−N unit, N(5)−Ru(1)−N(10) 171.6(2)° and N(11)−Ru(2)−N(16) 173.1(2)°. Bond angles between ligands in cis are in the range 85.2(2)−96.3(3)° for Ru(1) and 85.7(3)−95.4(3)° for Ru(2). Imidazolyl and pyridyl rings in the chelating NHC ligands form dihedral angles of 53.67(38)° and 62.07(33)°, respectively. The dihedral angles for the alignment between the imidazolyl rings and the pyrazolyl rings in trans to them are 11.07(87)° and 7.92(81)°, whereas the analogous angles for the pyridyl rings are 8.53(53)° and 6.01(49)°. The dinitrogen bridge ligand

dx.doi.org/10.1021/ic302553z | *Inorg. Chem.* 2013, 52, 4396−4410

Scheme 3

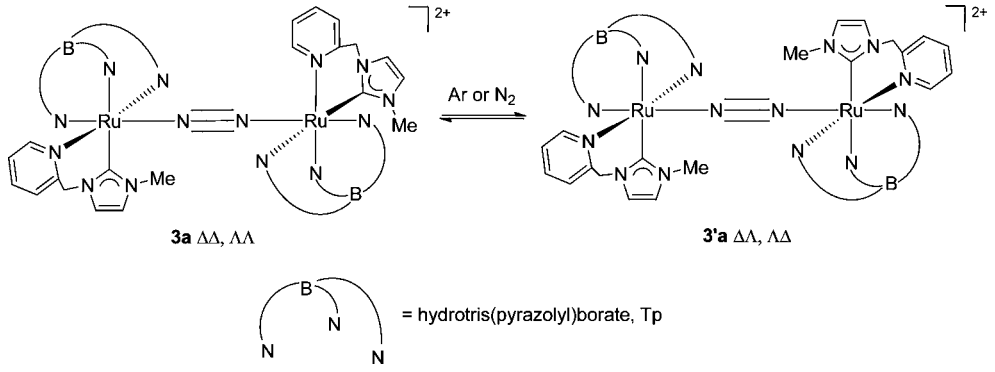

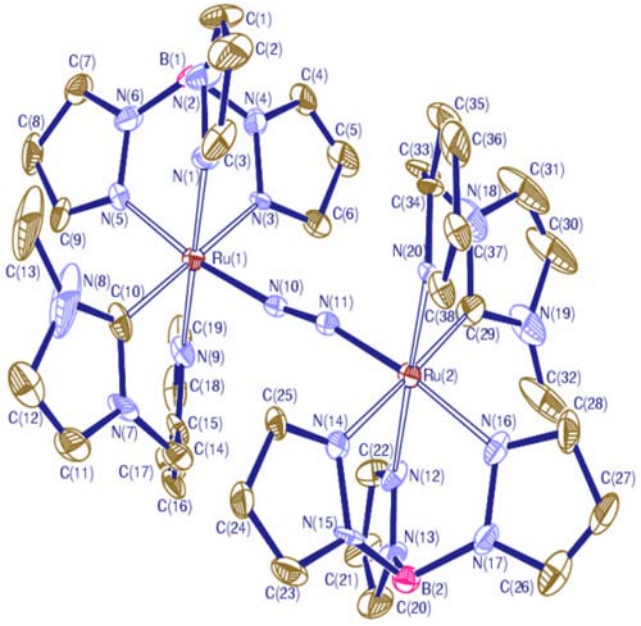

Figure 5. ORTEP diagram for $[\{TpRu(\kappa^2\text{-}C,N\text{-picolyl-}^{Me}I)\}_2(\mu\text{-}N_2)]^{2+}$ (picolyl-^{Me}I = 3-methyl-1-(2-picolyl)imidazol-2-ylidene) in **3′a** with 30% probability ellipsoids. Hydrogen atoms have been omitted for clarity. Color code: Ru, dark red; N, blue; C, brown; B, pink.

shows Ru−N bond lengths of 1.971(6) and 1.884(6) Å. These results are similar to the values found for the related complex $[\{TpRuCl(PCy_3)\}_2(\mu\text{-}N_2)]$.[28] Also, the N−N bond length, 1.124(5)Å, matches the mean value of 1.125(14) Å found for N≡N ligand bridging two Ru atoms.[33] Like in the case of the previously reported structures of **1b**, **2a**, and **2d**, the carbenic C exhibits the largest trans influence, while the shortest Ru−N distances, 2.035(6) Å for Ru(1) and 2.081(6) Å for Ru(2), correspond to the N atoms opposite to N_2 bridge ligand.

Consistently with the centrosymmetrical nature of the binuclear dinitrogen complex cations, the IR spectra of the mixture lack a band attributable to $\nu(N_2)$. However, the mixture displayed activity in Raman, showing a medium-weak band at 2091 cm^{-1}; considering the similarities in both structures, it is likely to find a coincidental value for $\nu(N_2)$. The Raman band can be assigned to the symmetric $\nu(N_2)$ mode, similar to those found for the symmetrical binuclear complexes $[\{(\eta^5\text{-}C_5H_5)Ru(dippe)\}_2(\mu\text{-}N_2)]^{2+}$ (2050 cm^{-1}),[19d] $[\{(\eta^5\text{-}C_5H_5)Ru(PEt_3)\}_2(\mu\text{-}N_2)]^{2+}$ (2064 cm^{-1}),[19d] $[\{Ru(acac)_2(P^iPr_3)\}_2(\mu\text{-}N_2)]$ (2089 cm^{-1}),[34] $[\{Ru(NH_3)_5\}_2(\mu\text{-}N_2)]^{4+}$ (2100 cm^{-1}),[35] and $[\{Ru(H_2O)_5\}_2(\mu\text{-}N_2)]^{4+}$ (2080 cm^{-1}).[36]

In addition, **3a** and **3′a** demonstrated to be moderately stable, for days, in the solid state toward air exposure. Furthermore, ^{1}H NMR spectra experiments were performed under argon and nitrogen atmosphere, to evaluate if an equilibrium with the terminal mononuclear dinitrogen complex was observed, according to eq 1 or 2, depending on the case. However, no evidence of the presence of a third species was found. In solution, the mixture of isomers remained unchanged. Also, freeze−pump−thaw degassing experiments showed no evidence of generation of unsaturated species or nitrogen loss.

$$[\{TpRu(\kappa^2-C,N-\text{picolyl}-^R\text{I})\}_2(\mu\text{-}N_2)]^{2+} \overset{Ar}{\rightleftharpoons} [TpRu(\kappa^2-C,N-\text{picolyl}-^R\text{I})(N_2)]^{+} + [TpRu(\kappa^2-C,N-\text{picolyl}-^R\text{I})]^{+} \quad (1)$$

$$[\{TpRu(\kappa^2-C,N-\text{picolyl}-^R\text{I})\}_2(\mu\text{-}N_2)]^{2+} + N_2 \rightleftharpoons 2[TpRu(\kappa^2-C,N-\text{picolyl}-^R\text{I})(N_2)]^{+} \quad (2)$$

Exposure of a fluorobenzene solution of **1b** and $NaBAr^F{}_4$ to 1 atm of N_2 at room temperature revealed the formation of the corresponding binuclear dinitrogen bridged complex, $[\{TpRu(\kappa^2\text{-}C,N\text{-picolyl-}^{iPr}I)\}_2(\mu\text{-}N_2)][BAr^F{}_4]_2$, **3b**. The new complex was isolated in ca. 93% yield as yellow crystals. Complex **3b** was characterized using ^{1}H and $^{13}C\{^1H\}$ NMR, IR, Raman, and elemental analysis. In contrast to **1a**, the isopropyl derivative, **1b**, led to a single isomer as evidenced by the NMR spectra, where no duplication of signals is observed. A distinctive Ru−C_2−NHC carbon resonance was observed at 178.3 ppm, in addition to a single characteristic pair of methylene group doublets in the ^{1}H NMR spectrum at 4.56 and 4.23 ppm, respectively. The NMR spectrum of **3b** was recorded under argon and nitrogen atmospheres; in neither case, the dissociation equilibrium as described in eq 1 or 2 was evident. The occurrence of one diastereoisomer can be explained by the larger steric effect of the isopropyl wingtip group, which must favor only one structure. The recrystallization of **3b** proved to be very challenging because despite working with numerous solvent mixtures, in no case were the crystals obtained large enough to perform an X-ray diffraction study. Besides, $\nu(N_2)$ band of **3b** in the solid state and in solution is inactive in the IR, but a medium-weak absorption band was observed in the Raman spectrum at 2093 cm^{-1}, as expected for a centrosymmetrical $\nu(N_2)$ band. Also, elemental analysis is consistent with the formation of the dinitrogen bridged complex.

dx.doi.org/10.1021/ic302553z | Inorg. Chem. 2013, 52, 4396−4410

In the case of **1c**, we were unable to synthesize the dinitrogen derivative. Many attempts of the reaction of the fluorobenzene solution of **1c** in the presence of $NaBAr^F{}_4$, at room temperature, low temperatures, and with different reaction times, were completed and proved to be unsuccessful. ^{1}H NMR spectra of the reaction mixtures showed evidence of decomposition products and the presence of some paramagnetic impurities in all cases. However, we continue to study the influence of picolyl−NHC ligands in the coordination of dinitrogen to the new TpRu fragment. The ruthenium complex bearing a phenyl group in the imidazolydene ligand, **1d,** was the next substrate and the obtained results were unexpected. ^{1}H NMR spectrum of the reaction mixture showed a mixture of three complexes, as evidenced by the triple set of doublets corresponding to the methylene bridged carbons of the picolyl-^{Ph}I ligands, as observed in Figure 6. It was plausible to

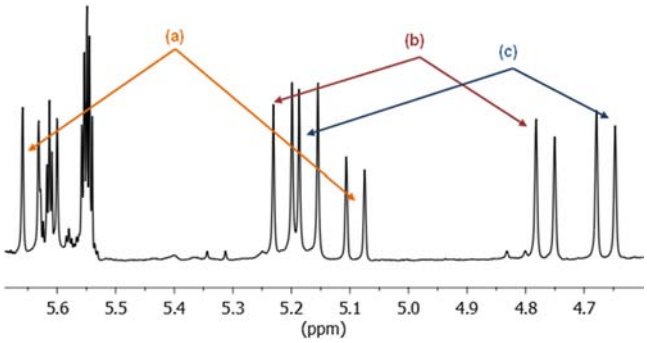

Figure 6. ^{1}H NMR (δ, CD_3NO_2) spectrum of the reaction mixture under dinitrogen before recrystallization: (a) mononuclear $[TpRu(\kappa^2\text{-}C,N\text{-picolyl-}^{Ph}I)(N_2)]^+$, **3″d;** (b) **3d**; and (c) **3′d**.

assume that two compounds in the mixture corresponded to the dinitrogen bridged diastereoisomers, **3d** and **3′d**, and the third species could be the mononuclear TpRu nitrogen complex, **3″d** (Scheme 4). The IR band corresponding to the asymmetrical $\nu(N_2)$ stretching at 2166 cm^{-1} confirmed the presence of a mononuclear terminal dinitrogen complex, **3″d**, as part of the mixture.

However, the dinitrogen bridged complex, **3′d**, was obtained almost quantitatively as yellow crystals after recrystallization. The IR $\nu(N_2)$ band was inactive in line with a centrosymmetrical complex, and in contrast to methyl and isopropyl derivatives cases, attempts of recording Raman spectra of **3′d** were unsuccessful due to the thermal decomposition of the product by the laser. Crystals of **3′d** suitable for X-ray diffraction studies were obtained from Et_2O/petroleum ether (1/2). ORTEP diagram of $[\{TpRu(\kappa^2\text{-}C,N\text{-picolyl-}^{Ph}I)\}_2(\mu\text{-}N_2)][BAr^F{}_4]_2$ complex, **3′d**, is displayed in Figure 7.

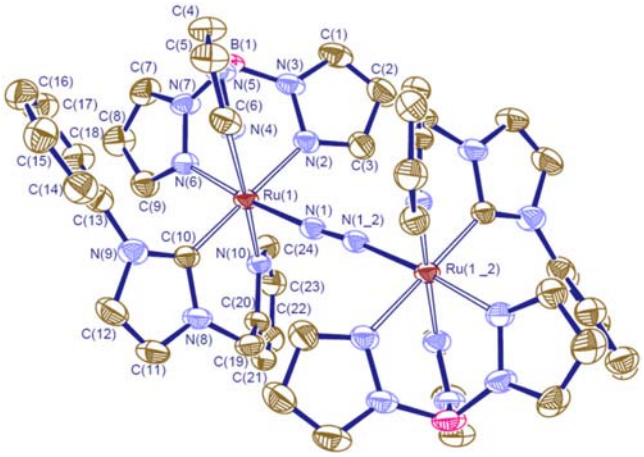

Figure 7. ORTEP diagram of the cation $[\{TpRu(\kappa^2\text{-}C,N\text{-picolyl-}^{Ph}I)\}_2(\mu\text{-}N_2)]^{2+}$ (picolyl-^{Ph}I = 3-phenyl-1-(2-picolyl)imidazol-2-ylidene) in **3′d** with 50% probability ellipsoids. Hydrogen atoms have been omitted for clarity. Color code: Ru, dark red; N, blue; C, brown; B, pink.

Since the asymmetric unit contains half of the cation $[\{TpRu(\kappa^2\text{-}C,N\text{-picolyl-}^{Ph}I)\}_2(\mu\text{-}N_2)]^{2+}$, the environment of

Scheme 4

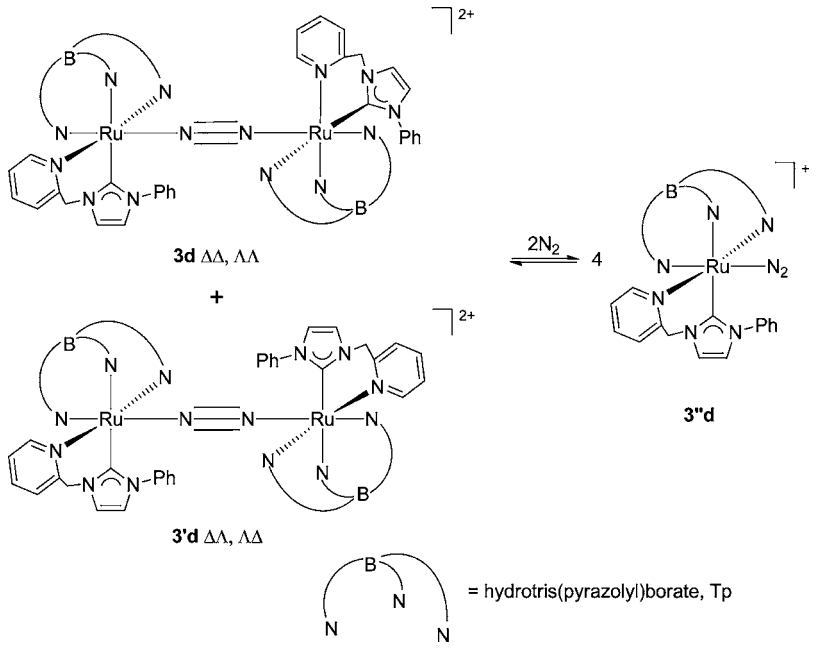

dx.doi.org/10.1021/ic302553z | Inorg. Chem. 2013, 52, 4396−4410

Scheme 5

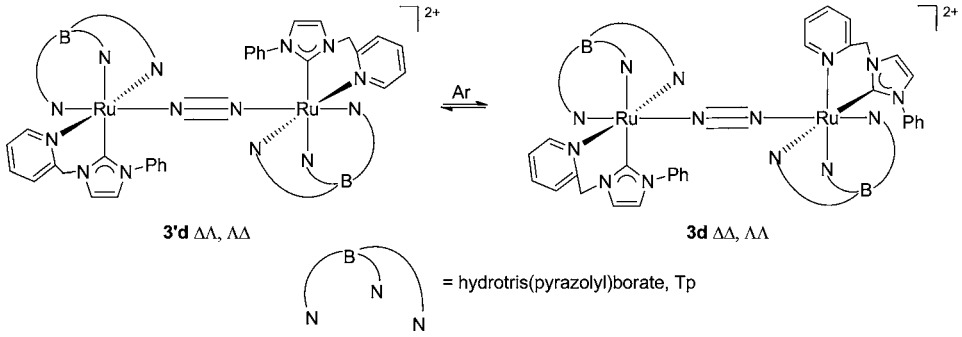

one Ru atom is repeated by symmetry. Like previously described crystal structures in this work, **3′d** shows ruthenium in a distorted octahedral geometry. As in complex **3′a**, the largest deviation from linearity is found in the N−Ru−N≡N−Ru−N unit, N(1)−Ru(1)−N(6) 173.59(14)°. Bond angles between ligands in cis are in the range 85.15(14)−95.13(15)°. Imidazolyl and pyridyl rings in the chelating NHC ligands form a dihedral angle of 47.08(18)°. The dihedral angle for the alignment between the imidazolyl ring and the pyrazolyl ring in trans to it is 18.81(11)°, whereas the analogous angle for the pyridyl ring is 13.14(20)°. The dinitrogen bridge ligand binds to Ru with a bond length of 1.941(3) Å. All these values are comparable with those found for **3′a**. Also, the carbenic C exhibits the largest trans influence, Ru(1)−N(2) 2.126(4) Å, while the shortest Ru−N distance, Ru(1)−N(6) 2.058(3) Å, corresponds to the N atom opposite to N_2 bridge ligand. However, in contrast to **3′a**, the value of 1.103(6) Å for the N−N bond length is in the lower quartile for the reported N≡N ligand bridging two Ru atoms.[33]

The NMR spectra of a freshly prepared solution of **3′d** yellow crystals recorded under argon atmosphere showed the presence of approximately 91% of this diastereoisomer. The characteristic signal corresponding to the Ru−C_2−NHC carbon atom appeared at 179.8 ppm, and the methylene bridge protons appeared as the expected pair of doublets at 4.60 and 4.18 ppm, respectively. However, in the course of 24 h at room temperature, an isomerization process to an equivalent mixture of diastereoisomers was observed (Scheme 5). The appearance of another diastereoisomer was confirmed by the decreasing of the ^{1}H NMR signals corresponding to **3′d** and the formation of the new complex **3d** (Figure 8).

When the NMR sample of **3′d** crystals was prepared under N_2 atmosphere, three species were detected, as in the case of the reaction mixture, showing the presence of both diastereoisomers and a third compound, the mononuclear dinitrogen complex, **3″d**. This behavior can be rationalized considering the process under nitrogen as dissociation equilibrium, according to eq 2. The ^{1}H NMR spectrum showed three typical sets of methylene bridged doublets (Figure 6). Also, the ^{13}C{^{1}H} NMR spectrum showed three signals corresponding to Ru−C_2−NHC chemicals shifts at 179.9, 179.8, and 190.2 ppm, belonging to **3d**, **3′d**, and **3″d**, respectively. Also, the NMR sample generated under nitrogen atmosphere was freeze−pump−thaw degassed and placed under argon to record the ^{1}H NMR spectra again. In this case, no changes in the ^{1}H NMR spectrum of the mixture were observed. When the sample prepared under argon was freeze−pump−thaw degassed and exposed to 1 atm of nitrogen, the equilibrium between dinitrogen bridged complexes and the

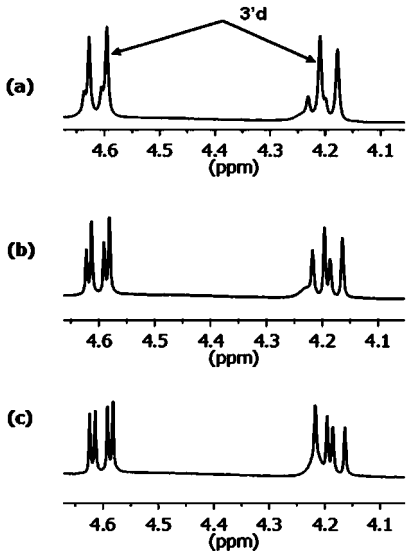

Figure 8. ^{1}H NMR (δ, CD_2Cl_2) spectra recorded at different times for the isomerization equilibrium, **3′d** ⇌ **3d**: (a) 30 min; (b) 12 h; and (c) 24 h.

mononuclear dinitrogen complex was reached upon several hours. The equilibrium constant K_{eq} for the process described in eq 2 and its dependence with temperature has been determined by measuring the concentration of **3d**, **3′d**, and **3″d** in a nitromethane-d_3 solution under dinitrogen at different temperatures, ranging from −15 to 30 °C. This led to a value of K_{eq} = 3.4 at 25 °C. A van′t Hoff plot (Figure S2 in Supporting Information) allowed the calculation of $\Delta H°$ and $\Delta S°$ for the process, and the corresponding values are 4.6 ± 0.2 kJ mol^{-1} and 27 ± 1 J mol^{-1} K^{-1}, respectively. These data suggest that the reaction in eq 2 is entropy driven, and therefore, at high temperatures, the equilibrium favors the formation of the mononuclear dinitrogen complex, **3″d**, whereas the dinitrogen dimers formation, **3d** and **3′d**, is favored by lowering the temperature.

It is interesting that one isomer, **3′d**, crystallized preferentially and that, in solution under dinitrogen atmosphere, it slowly transformed into a mixture of diastereoisomers, **3d** and **3′d**, and the mononuclear dinitrogen complex, **3″d**, via a dissociation equilibrium. Similar dissociation patterns of bridging dinitrogen compounds have been observed for a ruthenium(II) complex, *cis*-[{Ru(acac)$_2$(P^{i}Pr$_3$)}$_2$(μ-N$_2$)],[34] and an osmium(II) complex, *cis*-[{OsCl(bipy)$_2$}$_2$(μ-N$_2$)],[37] although no mononuclear species were detected in those cases. However, the nickel(0) complex, [{Ni(PCy$_3$)$_2$}$_2$(μ-N$_2$)],

dx.doi.org/10.1021/ic302553z | Inorg. Chem. 2013, 52, 4396−4410

dissociation equilibrium allowed the detection of the mononuclear species, $[Ni(PCy_3)_2(N_2)]$, by IR spectroscopy.[38]

The benzoimidazol derivative, **1e**, reactivity toward nitrogen proved to be similar to the **1d** analogue. The reaction of the fluorobenzene solution of **1e** and $NaBAr^F_4$ under 1 atm of N_2 generated a mixture of the diastereoisomers $[\{TpRu(\kappa^2\text{-}C,N\text{-picolyl-}^{Me}BI)\}_2(\mu\text{-}N_2)]^{2+}$, **3e** and **3′e**, corresponding to the nitrogen bridged complexes, in addition to the mononuclear terminal nitrogen compound $[TpRu(\kappa^2\text{-}C,N\text{-picolyl-}^{Me}BI)(N_2)]^+$, **3″e**. The mixture was characterized by NMR and IR spectroscopy. Particularly, the IR spectrum of the solid obtained from the reaction showed a strong absorption IR band at 2172 cm^{-1}, indicating the presence of $\nu(N_2)$ stretching frequencies as a consequence of the occurrence of the mononuclear complex, **3″e**. The ^1H NMR spectrum showed three typical sets of methylene bridged doublets as shown in Figure 9. Also, the $^{13}C\{^1H\}$ NMR spectrum showed three

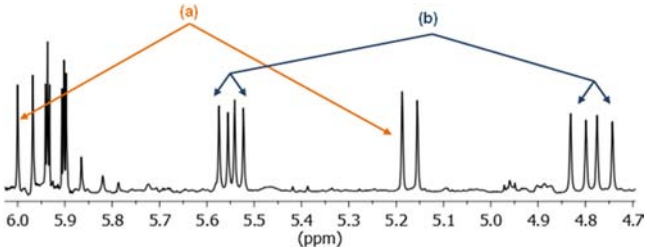

Figure 9. ^1H NMR (δ, CD_3NO_2) spectrum of the reaction product: (a) mononuclear $[TpRu(\kappa^2\text{-}C,N\text{-picolyl-}^{Me}BI)(N_2)]^+$, **3″e**; (b) **3e** and **3′e**.

signals corresponding to Ru−C_2−NHC chemicals shifts at 195.8, 195.9, and 205.9 ppm, belonging to **3e**, **3′e**, and **3″e**, respectively. Attempts of recording the Raman spectrum were unsuccessful due to sample decomposition by the laser.

The equilibrium constant K_{eq} for the process described in eq 2 using the benzoimidazolydene derivative and its dependence with temperature has been determined by measuring the concentration of **3e**, **3′e**, and **3″e** in a nitromethane-d_3 solution under dinitrogen at different temperatures, ranging from −15 to 30 °C. This led to a value of K_{eq} = 2.2 at 25 °C. A van′t Hoff plot (Figure S3 in Supporting Information) allowed the calculation of $\Delta H°$ and $\Delta S°$ for the process and the corresponding values are 6.8 ± 0.4 kJ mol^{-1} and 30 ± 2 J mol^{-1} K^{-1}, respectively. These data suggest, as in the case of the phenyl derivative, that the reaction is entropy driven favoring the formation of the mononuclear dinitrogen complex, **3″e**, at high temperatures.

No major differences were observed in terms of the donor properties of the picolyl−NHC ligands on the TpRu metal center, based on the CO stretching values of the carbonyl derivatives (Table 1). However, it is clear that the reactivity toward nitrogen is dramatically influenced by the picolyl−NHC ligands used. The same reaction conditions led to an equimolar mixture of nitrogen bridging diastereoisomers, as was the case for **1a**, or a single diastereoisomer when **1b** was used as starting material. Complex **1c** did not allow the isolation of any dinitrogen derivative, while **1d** and **1e** led to a mixture of the bridging diastereoisomers and the terminal nitrogen mononuclear complex in solution. It is likely that steric effects play a big role, when the generation of the nitrogen derivatives takes place. Furthermore, the occurrence of different diastereoisomers can be justified by the formation of prochiral pentacoordinated 16-electron species with a two legs piano stool geometry, $[TpRu(\kappa^2\text{-}C,N\text{-picolyl-NHC})]^+$. Steric effects may affect the equilibrium of the unsaturated species, which implies that, for different imidazol wingtips, it is unlikely to obtain the same mixture of complexes. The case of the benzoimidazol derivative is particular, considering the rigidity of the ligand benzoimidazolydene in comparison with the imidazolydene analogue, which might explain the differences observed in terms of the generated dinitrogen complexes. Also, it is interesting that these nitrogen derivatives are labile and may be used as catalysts in several transformations. We are currently investigating the catalytic applications of these new complexes.

Additionally, our group has reported the reactivity of Tp−ruthenium(II) phosphine complexes, but no similar equilibrium behavior was observed because the terminal mononuclear derivatives were obtained in all cases.[39] Only when cyclopentadienyl ruthenium(II) phosphine complexes were used as starting products some dinitrogen bridging complexes were generated.[19d]

Reactivity of Dinitrogen Complexes 3a, 3′a, and 3b with CO and CH_3CN. The reactivity of **3a**, **3′a**, and **3b** toward stronger donor ligands such as CO or CH_3CN led to the corresponding substitution derivatives, **2a−b** and **4a−b** (Scheme 6). The ^1H and $^{13}C\{^1H\}$NMR spectra of **4a−b**

Scheme 6

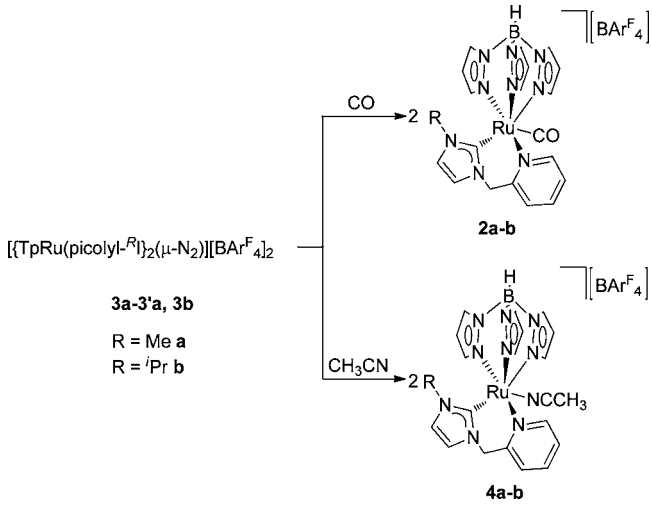

showed the typical characteristics of a coordinated CH_3CN ligand with a singlet proton resonance of integral three at 2.20 and 2.21 ppm, for **4a** and **4b**, respectively, as well as a coincidental carbon resonance at 3.93 ppm. The acetonitrile derivatives were also characterized by elemental analysis. Furthermore, **4a−b** were synthesized by treatment of a fluorobenzene solution of **1a−b** with $NaBAr^F_4$ in the presence of acetonitrile.

Reactivity of 1a−e with H_2. Several attempts of binding H_2 into the vacant coordination site at room temperature and lower temperatures failed to yield the desired products. The expected dihydrogen complexes were not synthesized in any case, but many decomposition products were observed in the reaction mixtures, presumably due to the instability of the in situ generated unsaturated TpRu 16-electron species. Additionally, the reaction under dihydrogen atmosphere was carried out in the presence of a base (ie. NaOH or KO^{t}Bu) to afford

dx.doi.org/10.1021/ic302553z | Inorg. Chem. 2013, 52, 4396−4410

the corresponding Ru−hydride derivatives, but in no case were the expected products obtained.

Reactivity of 1a−e with CH_2=CH_2. The coordination of olefins to transition metal complexes has attracted much attention, given the fact that the activation of olefins is a key step in several catalytic processes. Recently, Gunnoe and co-workers have reported the participation of an ethylene intermediate when TpRu(L)(NCMe)Ph (L = 2,6,7-trioxa-1-phosphabicyclo[2,2,1]heptanes, PMe_3, $P(pyr)_3$, $P(OCH_2)_3CEt$) complexes are used as catalysts in olefin hydroarylation reactions.[40] Also, Delaude and co-workers described the synthesis and catalytic applications of homo-bimetallic ruthenium−arene complexes bearing phosphine or NHC ligands starting from a ruthenium−ethylene complex.[41] Furthermore, Severin and co-workers reported the use of dinuclear ruthenium−ethylene complexes and its application in atom transfer radical addition (ATRA) and atom transfer radical polymerization (ATRP) reactions.[42] Thus, we decided to study the reactivity of the new ruthenium(II) picolyl−NHC complexes **1a−e** toward ethylene.

A fluorobenzene solution of **1a** and $NaBAr^F_4$ under ethylene atmosphere was stirred at room temperature for an hour. The resulting orange solid proved to be the ethylene derivative **5a**, [TpRu(κ^2-*C*,*N*-picolyl-^{Me}I)(η^2-CH_2CH_2)][BAr^F_4], obtained in 88% yield and characterized using ^{1}H NMR, $^{13}C\{^1H\}$ NMR, and elemental analysis. This compound is stable in solution under Ar atmosphere, and the coordination of ethylene proved to be irreversible, considering that no differences in the NMR spectra were observed after freeze−pump−thaw degassing the sample. The protons of the C_2H_4 ligand appeared in the ^{1}H NMR spectrum as two multiplets at 4.07 and 3.68 ppm, respectively. The ethylene carbon atoms appeared as one singlet at 71.3 ppm in the $^{13}C\{^1H\}$ NMR spectrum. This signal was observed for the half-sandwich cationic complexes [(η^5-C_5H_5)Ru($Ph_2PCH_2CH_2Im$)(η^2-CH_2CH_2)]$^+$,[43] [(η^5-C_5Me_5)-Ru(η^2-C_2H_4)(CO)(PMe^iPr_2)]$^+$,[44a] [(η^5-C_5Me_5)Ru(η^2-C_2H_4)-(dippe)]$^+$,[44b] [(η^5-C_5H_5)Ru(η^2-C_2H_4)(dippe)]$^+$,[44b] and [(η^5-C_5Me_5)Ru(η^2-C_2H_4)(P∼O)$_2$]$^+$,[44c] at higher field, 37.3, 47.3, 39.9, 33.3, and 46.9 ppm, respectively, indicating the presence of a C=C bond with stronger double bond character in the TpRu complex, **5a**. Continuing the reactivity study, a fluorobenzene solution of the isopropyl analogue, **1b**, and $NaBAr^F_4$ under ethylene atmosphere was allowed to react at room temperature for an hour. The η^2-ethylene derivative, **5b**, was obtained in almost quantitative yield, 97%, as yellow crystals. Complex **5b** was characterized using NMR spectroscopy, and as in the case of **5a**, the main spectroscopic characteristic is the low field $^{13}C\{^1H\}$ NMR shift of the ethylene carbon at 70.8 ppm. Furthermore, X-ray quality crystals were obtained by slow diffusion of petroleum ether into a concentrated diethyl ether solution. The ORTEP diagram of **5b** is displayed in Figure 10.

In this complex, Ru(II) has a distorted octahedral geometry where the dihapto ethylene ligand formally occupies one coordination site. The angle N(5)−Ru(1)−(ethylene centroid) is 178.87(11)° and other ligands form angles with the ethylene centroid in the range 93.35(19)−94.6(2)°. Also, the greatest deviation from linearity is found in the axis N(1)−Ru(1)−N(9) 170.89(12)°, and bond angles between ligands in cis range from 84.07(12)° to 98.29(13)°. Imidazolyl and pyridyl rings in the chelating NHC ligand form a dihedral angle of 54.47(16)°. In comparison with other cases discussed in this Article, the steric hindrance of ethylene ligand causes a worse alignment of

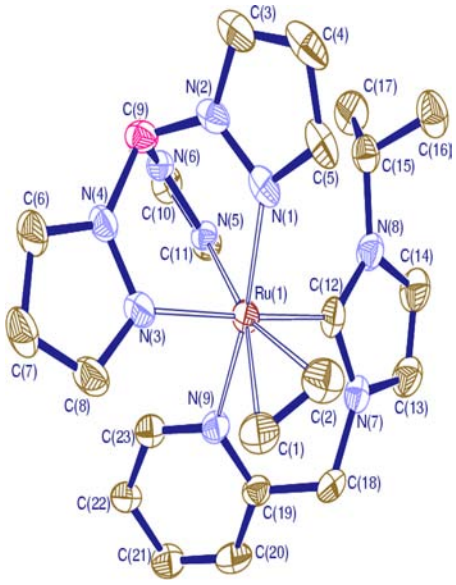

Figure 10. ORTEP diagram of the cation [TpRu(κ^2-*C*,*N*-picolyl-^{iPr}I)-(η^2-CH_2=CH_2)]$^+$ (picolyl-^{iPr}I = 3-isopropyl-1-(2-picolyl)imidazol-2-ylidene) in **5b** with 50% probability ellipsoids. Hydrogen atoms have been omitted for clarity. Color code: Ru, dark red; N, blue; C, brown; B, pink.

these rings with the pyrazolyl rings trans to them, showing dihedral angles of 22.98(22)° for the imidazolyl ring and 16.38(14)° for the pyridyl ring. The distance Ru(1)−(ethylene centroid) is 2.126(5) Å. Ru−N bond lengths increase from 2.068(3) Å for N(5) trans to η^2-CH_2=CH_2 to 2.154(3) Å for N(3) trans to the imidazol-2-ylidene carbon C(12). As in the other structures reported in this work, the carbenic NHC carbon exhibits the largest trans influence. Although some structures of CpRu and Cp*Ru with dihapto-ethylene have been described, there are no structures of TpRu with this ligand. The distance C(1)−C(2) 1.346(6) Å indicates less relaxation of the double bond in comparison with other mono π-olefins linked to the TpRu fragment.[45]

Following the synthesis of complexes **5a−b**, several attempts of obtaining the ethylene derivatives of **1c−e** were completed. However, in no case was it possible to obtain an isolable product. NMR spectra of the reaction mixtures showed the presence of several compounds as well as some paramagnetic impurities.

Reactivity of 1a−e with S_8. The interest in transition-metal complexes with sulfur containing ligands has increased due to their application as model compounds for biological systems. Our group has reported the reactivity of cyclopentadienyl ruthenium(II) complexes bearing phosphine ligands with H_2S and elemental sulfur.[46] Continuing the reactivity study toward small molecules, the next step was to use elemental sulfur. An excess of elemental sulfur was added to the fluorobenzene solutions of **1a−e** and $NaBAr^F_4$. The resulting solids were isolated after stirring the solutions for 1 h, filtering through a pad of Celite, and removing the solvent. The reaction mixtures were analyzed by NMR spectroscopy. However, only in the case of **1a** was a single product isolated, resulting in the formation of the disulfide complex [{TpRu(κ^2-*C*,*N*-picolyl-^{Me}I)}$_2$(μ-S_2)][BAr^F_4]$_2$, **6**. A few other disulfide ruthenium complexes have been reported, particularly using the method described by Rauchfuss and co-workers.[46,47] The ^{1}H NMR spectra of **6** is characteristic for centrosymmetrical

dx.doi.org/10.1021/ic302553z | *Inorg. Chem.* 2013, 52, 4396−4410

$\{TpRu(\kappa^2\text{-}C,N\text{-picolyl-}^{Me}I)\}_2$ moieties showing a single set of proton resonances. In the ^1H NMR spectrum, nine signals corresponding to the Tp ligand are observed, in addition to a set of doublets corresponding to the methylene bridge at 5.21 and 5.19 ppm, respectively. Also, the $^{13}C\{^1H\}$ NMR spectra showed the Ru−C_2−NHC chemical shift at 174.3 ppm. It is interesting that in the case of disulfide complex no isomerization is observed, in comparison with the dinitrogen-bridged analogues. Furthermore, crystals of **6** suitable for X-ray diffraction studies were obtained from slow diffusion of petroleum ether into a concentrated diethyl ether solution. The ORTEP diagram of **6** is displayed in Figure 11. This is the

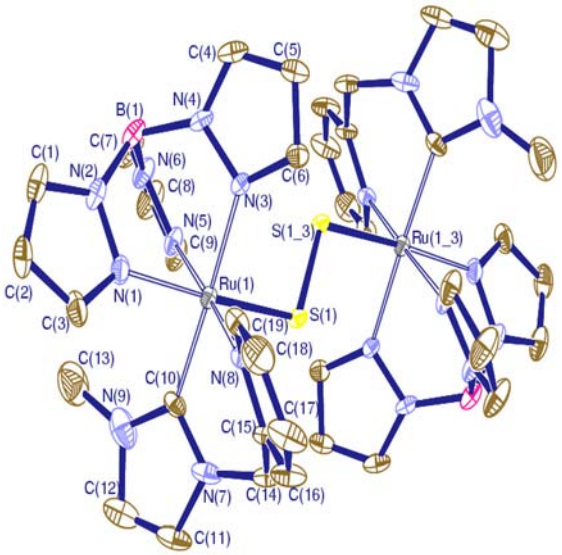

Figure 11. ORTEP diagram for $[\{TpRu(\kappa^2\text{-}C,N\text{-picolyl-}^{Me}I)\}_2(\mu\text{-}S_2)]^{2+}$ (picolyl-^{Me}I = 3-methyl-1-(2-picolyl)imidazol-2-ylidene) in **6** with 50% probability ellipsoids. Hydrogen atoms have been omitted for clarity. Color code: Ru, dark red; N, blue; C, brown; B, pink; S, yellow.

second disulfide ruthenium complex characterized crystallographically; previously, Amarasekara et. al reported the X-ray crystallographic analysis of $[\{(\eta^5\text{-}C_5H_5)Ru(PMe_3)_2\}_2(\mu\text{-}S_2)][SbF_6]_2$[47] and the first one bearing Tp and NHC ligands.

The structure of the divalent cation $[\{TpRu(\kappa^2\text{-}C,N\text{-picolyl-}^{Me}I)\}_2(\mu\text{-}S_2)]^{2+}$ shows a half repeated unit through the inversion center in the middle of the two S atoms. In contrast to other cases described in this work, the ruthenium atom shows a less distorted octahedral geometry, with axis ranging from N(5)−Ru(1)−N(8) 176.08(13)° to S(1)−Ru(1)−N(1) 176.83(10)°. In general, bond angles between ligands in *cis* are closer to the ideal value of 90°, in the interval 85.71(13)−95.06(16)°. In addition, imidazolyl and pyridyl rings in the chelating NHC ligands form a dihedral angle of 57.27(17)°. The alternating arrangement of the opposite ligand rings around ruthenium is even more regular than in the previous cases described in this work. The dihedral angle between the imidazolyl ring and the pyrazolyl ring in trans to it is 8.59(38)°, whereas the analogous angle for the pyridyl ring is 7.87(25)°, both lower than 10°. Also, the largest trans influence is exhibited by the carbenic C as evidenced by the largest Ru−N bond distance for Ru(1)−N(3), 2.110(3) Å. The disulfide bridge ligand binds Ru with a bond length of 2.218(1) Å, whereas the sulfur−sulfur distance is 1.987(2) Å, and the angle Ru(1)−S(1)−S(1_3) 109.16(7)° is close to the ideal tetrahedral value. All these values are similar to those reported for the related complex $[\{CpRu(PMe_3)_2\}_2(\mu_2\text{-}S_2)][SbF_6]_2$,[47] indicating an appreciable double-bond character for the μ-S_2 unit.

Reactivity of 1a−b with O_2. The activation of dioxygen by transition metal complexes has attracted significant interest considering the possible applications in many catalytic organic oxidation reactions.[48] Our recent work showed that $[(\eta^5\text{-}C_5Me_5)Ru(\kappa^2\text{-}C,N\text{-picolyl-}^{iPr}I)CH_3CN][BAr^F{}_4]$ in the presence of air afforded the η^2-dioxygen complex, $[(\eta^5\text{-}C_5Me_5)Ru(\kappa^2\text{-}C,N\text{-picolyl-}^{iPr}I)(\eta^2\text{-}O_2)][BAr^F{}_4]$.[24] In light of this and the work previously reported by Whittlesey and co-workers, regarding the formation of $[Ru(NHC)_4(\eta^2\text{-}O_2)H][BAr^F{}_4]$ and its reversible coordination,[49] the reaction of **1a−e** with $NaBAr^F{}_4$ as halide scavenger in the presence of air and dioxygen was investigated. The reactions were carried out in fluorobenzene at room temperature, and in all cases, an immediate color change from yellow−red to green/green−brown was observed. The ^1H NMR spectra of the reaction mixtures showed broad signals indicating the presence of paramagnetic species, generated after oxidation reactions. Crystallization of the reaction mixtures was attempted several times, but no material suitable for X-ray diffraction study was obtained.

CONCLUDING REMARKS

In continuation with our research with picolyl−NHC complexes of ruthenium, we have developed a high yield synthetic route to new hydrotris(pyrazolyl)borate ruthenium-(II) NHC complexes, **1a−e**. The complexes have been prepared using the transmetalation method from the in situ generated silver carbenes, with the appropriate imidazolium salts and silver oxide, and its reaction with [TpRu(COD)Cl]. In contrast to the ruthenium(II)−arene analogues previously generated by our group,[29] these transformation required high energy to complete the COD ligand substitution. Also, the crystal structure of **1b** has been determined. We have studied the influence of picolyl−NHC ligands in the ruthenium center, after systematically varying the imidazolydene ring N-wingtip and backbone substituents, via the synthesis and characterization of the carbonyl derivatives **2a−e**.

The reaction of the coordinatively unsaturated $[TpRu(\kappa^2\text{-}C,N\text{-picolyl-NHC})]^+$ species, generated in situ using $NaBAr^F{}_4$ as a halide scavenger, with small molecules indicated that the reactivity is strongly affected by the NHC wingtip and backbone substituents. $[TpRu(\kappa^2\text{-}C,N\text{-picolyl-}^{Me}I)]^+$ reacted with nitrogen to give an equimolar mixture of dinitrogen-bridged complexes, **3a** and **3′a**, while in the presence of ethylene atmosphere or elemental sulfur, led to the isolation of the TpRu η^2-ethylene derivative, **5a,** and the bridged TpRu disulfide complex, **6**, respectively. All complexes were spectroscopically characterized, and in the case of **3′a** and **6**, structurally characterized using X-ray diffraction. In contrast, $[TpRu(\kappa^2\text{-}C,N\text{-picolyl-}^{iPr}I)]^+$ reacted with nitrogen to give a single dinitrogen bridged complex, **3b**, and under ethylene atmosphere led to the isolation of the η^2-ethylene derivative, **5b.** However, $[TpRu(\kappa^2\text{-}C,N\text{-picolyl-}^{iPr}I)]^+$ failed to give any isolable product upon reaction with elemental sulfur. It is important to note that **5b** is the first example of a structurally characterized (via X-ray diffraction study) ethylene dihapto TpRu complex. The $[TpRu(\kappa^2\text{-}C,N\text{-picolyl-}^{Me}45DClI)]^+$ species decomposes upon exposure to all small molecules tested, except with CO, indicating the high instability of the

dx.doi.org/10.1021/ic302553z | *Inorg. Chem.* 2013, 52, 4396−4410

unsaturated complex. Also, [TpRu(κ^2-*C,N*-picolyl-^{Ph}I)]$^+$ reactivity toward nitrogen generated, after recrystallization, a single dinitrogen bridged complex, **3′d**, that in solution isomerizes to a mixture of diastereoisomers, **3d** and **3′d**, and the mononuclear nitrogen complex, **3″d**. Nevertheless, the phenyl derivative unsaturated complex decomposes upon exposure to ethylene and sulfur. The crystal structure of **3′d** has been obtained. Furthermore, [TpRu(κ^2-*C,N*-picolyl-^{Me}BI)]$^+$ in the presence of nitrogen led to a mixture of diastereoisomers, **3e** and **3′e**, and the mononuclear nitrogen complex, **3″e** in the solid state and in solution. Besides, the reactivity of **1e** proved to be similar to the case of the dichloro and phenyl derivative, failing to give an isolable product after reaction with ethylene and sulfur. The reactivity toward oxygen is independent of the picolyl−NHC ligands, **1a−e**, led to uncharacterizable oxidation products. The application of the new hydrotris(pyrazolyl)-borate ruthenium(II) picolyl-^{R}I derivatives generated with these labile ligands in different catalytic processes is ongoing.

Finally, it is important to note that, in all crystal structures reported in this work, the largest trans influence is exhibited by the carbenic carbon of the NHCs. This feature should be considered when studying their reactivity and catalytic applications.

EXPERIMENTAL SECTION

General Methods. Unless otherwise stated, all manipulations were carried out under dry nitrogen or argon using conventional Schlenk techniques. Tetrahydrofuran, diethyl ether, and petroleum ether (boiling range 40−60 °C) were obtained oxygen and water-free with an Innovative Technology Inc. solvent purification system. Acetonitrile, dichloromethane, dicholoroethane, and dimethylformamide were of anhydrous quality and used as received. All solvents were degassed immediately prior to use. 3-(Methyl)-1-(2-picolyl)imidazolium bromide (**a**),[50] 3-(isopropyl)-1-(2-picolyl)imidazolium bromide (**b**),[51] 3-(methyl)-1-(2-picolyl)benzoimidazolium bromide (**e**),[52] 3-phenyl-1-(2-picolyl)imidazolium bromide,[24] 3-methyl-1-(2-picolyl)-4,5-dichloroimidazolium bromide,[24] [TpRu(COD)Cl],[18f] and NaBAr$^F_4$[53] were prepared using slightly modified versions of the published procedures. All other reagents were purchased from commercial sources and used without further purification.

NMR spectra were recorded using Varian INOVA 400 MHz, Agilent 500, and Varian Inova 600 MHz spectrometers, and chemical shifts are reported relative to tetramethylsilane, $Si(CH_3)_4$, for ^1H and $^{13}C\{^1H\}$ signals. Assignments of ^1H and $^{13}C\{^1H\}$ NMR spectra were made on the basis of 2D NMR experiments. IR spectra were recorded in Nujol mulls with a Perkin-Elmer FTIR Spectrum 1000 spectrophotometer. Raman spectra were recorded with a BTWTec i-Raman spectrophotometer. Microanalyses were performed with a LECO CHNS-932 elemental analyzer by Servicios Centrales de Ciencia y Tecnología, Universidad de Cádiz. Synthesis and characterization data of selected compounds is presented in the experimental section.

Representative Procedure for Synthesis of TpRu(κ^2-*C,N*-picolyl-NHC)Cl Complexes 1a−e. A suspension of the appropriate picolyl imidazolium bromide (**a−e**) and silver oxide (1 equiv) in 1,2-dichloroethane was stirred at room temperature in the dark for 3 h. The resulting light yellow mixture was then filtered through a pad of Celite into a suspension of [TpRu(COD)Cl] in DMF and stirred at 150 °C for 5 h. The suspension color changed from light yellow to orange and was filtered through Celite to remove silver salts, and the solvent was removed under reduced pressure. The resulting solid was extracted with THF and filtered through a pad of Celite to remove the insoluble residues, and the solvent was removed under reduced pressure. The resulting solid was washed with ether, dried under vacuum, and recrystallized from CH_2Cl_2/hexane.

*[TpRuCl(κ^2-C,N-3-methyl-1-(2-picolyl)imidazol-2-ylidene)] (**1a**).* Transmetalation was carried out in 1,2-dichloroethane (15 mL) with 1-methyl-3-picolylimidazolium bromide **a** (381.2 mg, 1.5 mmol), Ag_2O (173.8 mg, 0.75 mmol), and [TpRu(COD)Cl] (457.7 mg, 1.0 mmol) in DMF (15 mL). The product was an orange microcrystalline solid. Yield: 317.3 mg, 81%. ^1H NMR (CD_2Cl_2, 600 MHz): δ 7.82 (d, $^3J_{HH}$ = 2.30 Hz, 1H, H_{Tp}), 7.76 (d, $^3J_{HH}$ = 2.49 Hz, 1H, H_{Tp}), 7.64 (d, $^3J_{HH}$ = 2.11 Hz, 1H, H_{Tp}), 7.62 (br s, 1H, H_{Tp}), 7.52 (br s, 1H, H_{Tp}), 7.49 (t, $^3J_{HH}$ = 7.68 Hz, 1H, $H_{pyridine}$), 7.47 (d, $^3J_{HH}$ = 5.57 Hz, 1H, $H_{pyridine}$), 7.36 (d, $^3J_{HH}$ = 7.67 Hz, 1H, $H_{pyridine}$), 7.22 (d, $^2J_{HH}$ = 15.06 Hz, 1H, H_{bridge}), 7.20 (d, $^3J_{HH}$ = 1.92 Hz, 1H, H_{imid}), 6.76 (d, $^3J_{HH}$ = 1.73 Hz, 1H, H_{imid}), 6.75 (t, $^3J_{HH}$ = 7.43 Hz, 1H, $H_{pyridine}$), 6.29 (vt, $^3J_{HH}$ = 2.02 Hz, 1H, H_{Tp}), 6.13 (vt, $^3J_{HH}$ = 2.03 Hz, 1H, H_{Tp}), 5.91 (vt, $^3J_{HH}$ = 2.02 Hz, 1H, H_{Tp}), 5.75 (br s, 1H, H_{Tp}), 5.00 (d, $^2J_{HH}$ = 14.39 Hz, 1H, H_{bridge}), 2.42 (s, 3H, NCH_3). $^{13}C\{^1H\}$ NMR (CD_2Cl_2, 150 MHz): δ 192.3 (C_{imid}Ru), 161.3 (C_{py}), 157.8 (C_{py}), 145.4 (Tp), 143.4 (Tp), 142.7 (Tp), 136.4 (Tp), 135.1 (Tp), 134.8 (Tp), 134.2 (C_{py}), 123.2 (C_{py}), 122.6 (C_{py}), 121.9 (C_{imid}), 121.5 (C_{imid}), 105.9 (Tp), 105.8 (Tp), 105.6 (Tp), 55.8 (CH_2), 35.0 (NCH_3). Anal. Calcd. for $C_{19}H_{21}BClN_9Ru$: C 43.65, H 4.05, N 24.11. Found: C 43.58, H 4.10, N 24.15.

*[TpRuCl(κ^2-C,N-3-isopropyl-1-(2-picolyl)imidazol-2-ylidene)]·0.8CH_2Cl_2 (**1b**).* Transmetalation was carried out in 1,2-dichloroethane (15 mL) with 1-isopropyl-3-picolylimidazolium bromide **b** (424.8 mg, 1.5 mmol), Ag_2O (173.8 mg, 0.75 mmol), and [TpRu(COD)Cl] (457.7 mg, 1.0 mmol) in DMF (15 mL). The product was a red microcrystalline solid. Yield: 326.4 mg, 79%. ^1H NMR (CD_2Cl_2, 600 MHz): δ 7.82 (d, $^3J_{HH}$ = 2.30 Hz, 1H, H_{Tp}), 7.76 (d, $^3J_{HH}$ = 2.30 Hz, 2H, H_{Tp}), 7.66 (d, $^3J_{HH}$ = 1.53 Hz, 1H, H_{Tp}), 7.64 (t, $^3J_{HH}$ = 7.57 Hz, 1H, $H_{pyridine}$), 7.60 (d, $^3J_{HH}$ = 1.72 Hz, 1H, H_{Tp}), 7.51 (d, $^3J_{HH}$ = 7.39 Hz, 1H, $H_{pyridine}$), 7.50 (d, $^3J_{HH}$ = 1.92 Hz, 1H, H_{imid}), 7.47 (d, $^3J_{HH}$ = 5.36 Hz, 1H, $H_{pyridine}$), 7.22 (d, $^3J_{HH}$ = 1.92 Hz, 1H, H_{imid}), 7.18 (d, $^2J_{HH}$ = 14.20 Hz, 1H, H_{bridge}), 6.88 (t, $^3J_{HH}$ = 6.67 Hz, 1H, $H_{pyridine}$), 6.23 (vt, $^3J_{HH}$ = 2.11 Hz, 1H, H_{Tp}), 6.12 (vt, $^3J_{HH}$ = 2.11 Hz, 1H, H_{Tp}), 5.99 (vt, $^3J_{HH}$ = 2.11 Hz, 1H, H_{Tp}), 5.94 (d, $^3J_{HH}$ = 1.54 Hz, 1H, H_{Tp}), 5.22 (d, $^2J_{HH}$ = 14.20 Hz, 1H, H_{bridge}), 3.08 (m, $^3J_{HH}$ = 6.71 Hz, 1H, CH), 1.00 (d, $^3J_{HH}$ = 6.52 Hz, 3H, CH_3), 0.66 (d, $^3J_{HH}$ = 6.72 Hz, 3H, CH_3). $^{13}C\{^1H\}$ NMR (CD_2Cl_2, 150 MHz): δ 191.4 (C_{imid}Ru), 162.7 (C_{py}), 158.2 (C_{py}), 146.6 (Tp), 144.6 (Tp), 143.1 (Tp), 136.5 (Tp), 135.7 (Tp), 134.8 (Tp), 134.7 (C_{py}), 123.7 (C_{py}), 123.1 (C_{py}), 123.1 (C_{imid}), 117.0 (C_{imid}), 106.4 (Tp), 105.9 (Tp), 105.5 (Tp), 55.6 (CH_2), 49.3 (CH), 24.8 (CH_3), 23.4 (CH_3). Anal. Calcd. for $C_{21}H_{25}BClN_9Ru$ + 0.8CH_2Cl_2: C 42.32, H 4.33, N 20.37. Found: C 42.27, H 4.28, N 20.41.

*[TpRu(κ^2-C,N-3-phenyl-1-(2-picolyl)imidazol-2-ylidene)(CO)]-[BAr$^F_4$]·0.5Et_2O (**2d**).* [TpRu(κ^2-*C,N*-picolyl-^{Ph}I)Cl] (117.0 mg, 0.2 mmol) and NaBAr$^F_4$ (177.2 mg, 0.2 mmol) were suspended in 6 mL of fluorobenzene under 1 atm of CO, and an orange−yellow solution was observed. The mixture was stirred for 1 h. The solvent was removed under reduced pressure. The solid was dissolved in Et_2O (10 mL) and filtered through a pad of Celite to remove NaCl. The resulting red solution was layered with petroleum ether to yield red crystals. Yield: 262.2 mg (91%). ^1H NMR (CD_3NO_2, 400 MHz): δ 8.08 (d, $^3J_{HH}$ = 2.0 Hz, 1H, H_{Tp}), 8.00 (t, $^3J_{HH}$ = 7.6 Hz, 1H, $H_{pyridine}$), 7.86 (br s, 9H, BAr$^F_4$ + H_{Tp}), 7.83 (d, $^3J_{HH}$ = 7.68 Hz, 1H, $H_{pyridine}$), 7.71 (d, $^3J_{HH}$ = 2.4 Hz, 1H, H_{Tp}), 7.68 (br s, 4H, BAr$^F_4$), 7.66 (d, $^3J_{HH}$ = 2.6 Hz, 1H, H_{imid}), 7.64 (d, $^3J_{HH}$ = 5.8 Hz, 1H, $H_{pyridine}$), 7.49 (d, $^3J_{HH}$ = 2.0 Hz, 1H, H_{Tp}), 7.24−7.21 (m, 2H, $H_{pyridine}$ + H_{imid}), 7.11 (d, $^3J_{HH}$ = 2.0 Hz, 1H, H_{Tp}), 7.03 (t, $^3J_{HH}$ = 7.3 Hz, 1H, H_{Ph}), 6.91 (t, $^3J_{HH}$ = 7.8 Hz, 2H, H_{Ph}), 6.79 (d, $^3J_{HH}$ = 1.5 Hz, 1H, H_{Tp}), 6.38 (vt, $^3J_{HH}$ = 2.2 Hz, 1H, H_{Tp}), 6.35 (d, $^3J_{HH}$ = 2.5 Hz, 1H, H_{Tp}), 6.33 (d, $^3J_{HH}$ = 7.3 Hz, 2H, H_{Ph}), 5.79 (d, $^2J_{HH}$ = 16.0 Hz, 1H, H_{bridge}), 5.74 (d, $^2J_{HH}$ = 16.0 Hz, 1H, H_{bridge}), 5.67 (m, 2H, H_{Tp}). $^{13}C\{^1H\}$ NMR (CD_3NO_2, 101 MHz): δ 204.6 (CO), 177.0 (C_{imid}Ru), 163.3 (q, $^1J_{B-C}$ = 50.0 Hz, BAr$^F_4$), 158.1 (C_{py}), 157.1 (C_{py}), 148.0 (Tp), 145.1 (Tp), 143.9 (Tp), 141.1 (C_{Ph}), 140.5 (C_{py}), 137.9 (Tp), 137.5 (Tp), 137.5 (Tp), 136.3 (BAr$^F_4$), 130.4 (q, $^2J_{C-F}$ = 28.7 Hz, BAr$^F_4$), 129.8 (C_{Ph}), 129.5 (C_{Ph}), 126.7 (C_{Ph}), 126.4 (C_{py}), 126.1 (C_{imid}), 126.1 (q, $^1J_{C-F}$ = 271.9 Hz, BAr$^F_4$), 124.1 (C_{py}), 119.0 (BAr$^F_4$), 108.5 (Tp), 108.2 (Tp), 108.0 (Tp), 57.7 (CH_2). IR (nujol, cm^{-1}) ν (CO) 1976. Anal. Calcd. for $C_{57}H_{35}B_2F_{24}N_9ORu$ + 0.5Et_2O: C 47.96, H 2.73, N 8.53. Found: C 47.88, H 2.76, N 8.49.

dx.doi.org/10.1021/ic302553z | Inorg. Chem. 2013, 52, 4396−4410

*[TpRu(κ²-C,N-3-methyl-1-(2-picolyl)benzoimidazol-2-ylidene)(CO)][BAr$^F_4$] (**2e**).* [TpRu(κ²-C,N-picolyl-^{Me}BI)Cl] (114.6 mg, 0.2 mmol) and NaBAr$^F_4$ (177.2 mg, 0.2 mmol) were suspended in 6 mL of fluorobenzene under 1 atm of CO, and a red solution was observed. The mixture was stirred for 1 h. The solvent was removed under reduced pressure. The solid was dissolved in Et_2O (10 mL) and filtered through a pad of Celite to remove NaCl. The resulting brown solution was layered with petroleum ether to yield brown crystals. Yield: 254.2 mg (89%). ^{1}H NMR (CD_3NO_2, 500 MHz): δ 8.06 (d, $^3J_{HH}$ = 2.4 Hz, 1H, H_{Tp}), 8.01 (d, $^3J_{HH}$ = 2.4 Hz, 1H, H_{Tp}), 7.99 (d, $^3J_{HH}$ = 2.4 Hz, 1H, H_{Tp}), 7.87 (br s, 8H, BAr$^F_4$), 7.84−7.79 (m, 3H, H_{Tp} + 2$H_{pyridine}$), 7.78 (d, $^3J_{HH}$ = 7.9 Hz, 1H, $H_{benzoimid}$), 7.71 (d, $^3J_{HH}$ = 5.5 Hz, 1H, $H_{pyridine}$), 7.68 (br s, 4H, BAr$^F_4$), 7.53 (d, $^3J_{HH}$ = 1.8 Hz, 1H, H_{Tp}), 7.38 (m, 1H, $H_{benzoimid}$), 7.30 (t, $^3J_{HH}$ = 7.6 Hz, 1H, $H_{benzoimid}$), 7.10 (t, $^3J_{HH}$ = 7.4 Hz, 1H, $H_{pyridine}$), 6.84 (d, $^3J_{HH}$ = 7.9 Hz, 1H, $H_{benzoimid}$), 6.47 (vt, $^3J_{HH}$ = 1.8 Hz, 1H, H_{Tp}), 6.33 (vt, $^3J_{HH}$ = 2.4 Hz, 1H, H_{Tp}), 6.16 (d, $^3J_{HH}$ = 1.8 Hz, 1H, H_{Tp}), 6.07 (vt, $^3J_{HH}$ = 1.8 Hz, 1H, H_{Tp}), 5.98 (d, $^2J_{HH}$ = 15.9 Hz, 1H, H_{bridge}), 5.17 (d, $^2J_{HH}$ = 16.5 Hz, 1H, H_{bridge}), 2.68 (s, 3H, NCH_3). ^{13}C{^{1}H} NMR (CD_3NO_2, 125 MHz): δ 205.9 (CO), 168.6 ($C_{benzoimid}$Ru), 163.2 (q, $^1J_{B-C}$ = 49.9 Hz, BAr$^F_4$), 160.0 (C_{py}), 158.2 (C_{py}), 147.6 (Tp), 146.1 (Tp), 144.9 (Tp), 138.5 (Tp), 138.3 (Tp), 137.9 ($C_{benzoimid}$), 137.7 (Tp), 137.2 (C_{py}), 136.2 (BAr$^F_4$), 136.1 ($C_{benzoimid}$), 130.3 (q, $^2J_{C-F}$ = 31.4 Hz, BAr$^F_4$), 126.0 (q, $^1J_{C-F}$ = 271.26 Hz, BAr$^F_4$), 125.61 (C_{py}), 125.3 (C_{py}), 123.7 ($C_{benzoimid}$), 123.5 ($C_{benzoimid}$), 119.0 (BAr$^F_4$), 110.5 ($C_{benzoimid}$), 109.6 ($C_{benzoimid}$), 108.4 (Tp), 107.9 (Tp), 107.8 (Tp), 51.6 (CH_2), 32.9 (NCH_3). IR (nujol, cm^{-1}) ν (CO) 1976. Anal. Calcd. for $C_{56}H_{35}B_2F_{24}N_9ORu$: C 47.08, H 2.47, N 8.82. Found: C 47.03, H 2.38, N 9.01.

*[{TpRu(κ²-C,N-3-methyl-1-(2-picolyl)imidazol-2-ylidene)}$_2$(μ-N$_2$)][BAr$^F_4$]$_2$ (**3a−3′a**).* [TpRu(κ²-C,N-picolyl-^{Me}I)Cl] (105.5 mg, 0.2 mmol) and NaBAr$^F_4$ (177.2 mg, 0.2 mmol) were suspended in 6 mL of fluorobenzene under 1 atm of N_2, and a dark yellow solution was observed. The mixture was stirred for 1 h. The solvent was removed under reduced pressure. The solid was dissolved in Et_2O (10 mL) and filtered through a pad of Celite to remove NaCl. The resulting yellow solution was layered with petroleum ether to yield yellow crystals. Yield: 496.7 mg (91%). ^{1}H NMR (CD_2Cl_2, 400 MHz): δ 7.97 (dd, $^3J_{HH}$ = 2.4, 0.6 Hz, 1H, H_{Tp}), 7.93 (m, 1H, H_{Tp}), 7.89 (m, 2H, H_{Tp}), 7.85 (m, 1H, $H_{pyridine}$), 7.80 (m, 2H, $H_{pyridine}$ + H_{Tp}), 7.74 (br s, 16H, BAr$^F_4$), 7.71 (m, 1H, $H_{pyridine}$), 7.57 (br s, 8H, BAr$^F_4$), 7.52 (m, 1H, $H_{pyridine}$), 7.38 (m, 1H, H_{Tp}), 7.24 (m, 2H, $H_{pyridine}$), 7.13 (t, $^3J_{HH}$ = 6.7 Hz, 1H, $H_{pyridine}$), 7.08 (d, $^3J_{HH}$ = 1.4 Hz, 1H, H_{Tp}), 7.05 (m, 1H, $H_{pyridine}$), 7.02 (d, $^3J_{HH}$ = 2.1 Hz, 1H, H_{imid}), 7.01 (d, $^3J_{HH}$ = 2.1 Hz, 1H, H_{imid}), 7.00 (d, $^3J_{HH}$ = 2.0 Hz, 1H, H_{Tp}), 6.91 (d, $^3J_{HH}$ = 1.9 Hz, 1H, H_{Tp}), 6.85 (d, $^3J_{HH}$ = 2.1 Hz, 1H, H_{imid}), 6.82 (m, 2H, H_{Tp} + H_{imid}), 6.39 (m, 1H, H_{Tp}), 6.29 (vt, $^3J_{HH}$ = 2.1 Hz, 1H, H_{Tp}), 6.25 (m, 1H, H_{Tp}), 6.20 (vt, $^3J_{HH}$ = 2.3 Hz, 1H, H_{Tp}), 6.13 (vt, $^3J_{HH}$ = 2.1 Hz, 1H, H_{Tp}), 6.10 (m, 2H, H_{Tp}), 6.03 (m, 1H, H_{Tp}), 5.83 (m, 1H, H_{Tp}), 4.58 (d, $^2J_{HH}$ = 16.3 Hz, 2H, H_{bridge}), 4.26 (m, 2H, H_{bridge}), 2.43 (s, 3H, NCH_3), 2.39 (s, 3H, NCH_3). ^{13}C{^{1}H} NMR (CD_2Cl_2, 101 MHz): δ 180.5 (C_{imid}Ru), 180.4 (C_{imid}Ru), 162.2 (q, $^1J_{B-C}$ = 50.2 Hz, BAr$^F_4$), 156.8 (C_{py}), 156.7 (C_{py}), 156.5 (C_{py}), 156.4 (C_{py}), 143.7 (Tp), 143.3 (Tp), 143.2 (Tp), 141.6 (Tp), 141.1 (Tp), 138.9 (C_{py}), 137.9 (C_{py}), 137.8 (Tp), 137.7 (Tp), 137.7 (Tp), 137.1 (Tp), 135.2 (BAr$^F_4$), 129.3 (q, $^2J_{C-F}$ = 32.8 Hz, BAr$^F_4$), 125.6 (C_{imid}), 125.6 (C_{imid}), 125.3 (C_{imid}), 125.3 (C_{imid}), 125.0 (q, $^1J_{C-F}$ = 275.9 Hz, BAr$^F_4$), 124.3 (C_{py}), 124.3 (C_{py}), 122.7 (C_{py}), 122.7 (C_{py}), 117.9 (BAr$^F_4$), 107.8 (Tp), 107.7 (Tp), 107.7 (Tp), 107.6 (Tp), 54.3 (CH_2), 54.3 (CH_2), 35.9 (NCH_3), 35.9 (NCH_3). Anal. Calcd. for $C_{102}H_{66}B_4F_{48}N_{20}Ru_2$: C 44.89, H 2.44, N 10.26. Found: C 44.85, H 2.46, N 10.28.

*[{TpRu(κ²-C,N-3-isopropyl-1-(2-picolyl)imidazol-2-ylidene)}$_2$(μ-N$_2$)][BAr$^F_4$]$_2$ (**3b**).* [TpRu(κ²-C,N-picolyl-^{iPr}I)Cl] (110.2 mg, 0.2 mmol) and NaBAr$^F_4$ (177.2 mg, 0.2 mmol) were suspended in 6 mL of fluorobenzene under 1 atm of N_2, and an orange solution was observed. The mixture was stirred for 1 h. The solvent was removed under reduced pressure. The solid was dissolved in Et_2O (10 mL) and filtered through a pad of Celite to remove NaCl. The resulting dark yellow solution was layered with petroleum ether to yield yellow crystals. Yield: 518.1 mg (93%). ^{1}H NMR (CD_2Cl_2, 400 MHz): δ 7.93−7.90 (m, 3H, H_{Tp}), 7.75 (br s, 8H, BAr$^F_4$), 7.72 (t, $^3J_{HH}$ = 7.6 Hz, 1H, $H_{pyridine}$), 7.57 (br s, 4H, BAr$^F_4$), 7.44 (d, $^3J_{HH}$ = 5.90 Hz, 1H, $H_{pyridine}$), 7.22 (d, $^3J_{HH}$ = 7.3 Hz, 1H, $H_{pyridine}$), 7.18 (d, $^3J_{HH}$ = 2.0 Hz, 1H, H_{imid}), 7.04 (m, 1H, $H_{pyridine}$), 7.01 (d, $^3J_{HH}$ = 2.0 Hz, 1H, H_{imid}), 6.86 (d, $^3J_{HH}$ = 1.8 Hz, 1H, H_{Tp}), 6.84 (d, $^3J_{HH}$ = 2.0 Hz, 1H, H_{Tp}), 6.18 (d, $^3J_{HH}$ = 2.0 Hz, 1H, H_{Tp}), 6.15 (vt, $^3J_{HH}$ = 2.2 Hz, 1H, H_{Tp}), 6.13−6.10 (m, 2H, H_{Tp}), 4.56 (d, $^2J_{HH}$ = 16.1 Hz, 1H, H_{bridge}), 4.23 (d, $^2J_{HH}$ = 16.1 Hz, 1H, H_{bridge}), 2.84 (m, 1H, CH), 0.93 (d, $^3J_{HH}$ = 6.8 Hz, 3H, CH_3), 0.67 (d, $^3J_{HH}$ = 6.8 Hz, 3H, CH_3). ^{13}C{^{1}H} NMR (CD_2Cl_2, 101 MHz): δ 178.3 (C_{imid}Ru), 162.1 (q, $^1J_{B-C}$ = 49.6 Hz, BAr$^F_4$), 156.7 (C_{py}), 156.5 (C_{py}), 144.1 (Tp), 143.6 (Tp), 140.96 (Tp), 138.9 (C_{py}), 138.1 (Tp), 137.1 (Tp), 135.2 (BAr$^F_4$), 129.3 (q, $^2J_{C-F}$ = 32.0 Hz, BAr$^F_4$), 125.6 (C_{py}), 125.2 (C_{py}), 125.0 (q, $^1J_{C-F}$ = 272.4 Hz, BAr$^F_4$), 123.5 (C_{imid}), 118.8 (C_{imid}), 117.9 (BAr$^F_4$), 107.7 (Tp), 107.5 (Tp), 107.4 (Tp), 54.2 (CH_2), 50.9 (NCH), 24.4 (CH_3), 22.1 (CH_3). Anal. Calcd. for $C_{106}H_{74}B_4F_{48}N_{20}Ru_2$: C 45.71, H 2.68, N 10.06. Found: C 45.80, H 2.74, N 9.99.

*Δ,Λ-[{TpRu(κ²-C,N-3-phenyl-1-(2-picolyl)imidazol-2-ylidene)}$_2$(μ-N$_2$)][BAr$^F_4$]$_2$·2Et$_2$O (**3′d**).* [TpRu(κ²-C,N-picolyl-^{Ph}I)Cl] (117.0 mg, 0.2 mmol) and NaBAr$^F_4$ (177.2 mg, 0.2 mmol) were suspended in 6 mL of fluorobenzene under 1 atm of N_2, and a dark yellow solution was observed. The mixture was stirred for 1 h. The solvent was removed under reduced pressure. The solid was dissolved in Et_2O (10 mL) and filtered through a pad of Celite to remove NaCl. The resulting yellow solution was layered with petroleum ether to yield yellow crystals. Yield: 573.6 mg (82%). ^{1}H NMR (CD_2Cl_2, 500 MHz): δ 7.91 (d, $^3J_{HH}$ = 2.3 Hz, 1H, H_{Tp}), 7.87 (d, $^3J_{HH}$ = 2.3 Hz, 1H, H_{Tp}), 7.77 (t, $^3J_{HH}$ = 7.8 Hz, 1H, $H_{pyridine}$),7.72 (br s, 8H, BAr$^F_4$), 7.55 (br s, 4H, BAr$^F_4$), 7.48 (d, $^3J_{HH}$ = 5.8 Hz, 1H, $H_{pyridine}$), 7.46 (d, $^3J_{HH}$ = 2.3 Hz, 1H, H_{Tp}), 7.24 (d, $^3J_{HH}$ = 7.5 Hz, 1H, $H_{pyridine}$), 7.12 (d, $^3J_{HH}$ = 2.2 Hz, 1H, H_{imid}), 7.10 (m, 1H, $H_{pyridine}$), 7.08 (d, $^3J_{HH}$ = 1.8 Hz, 1H, H_{imid}), 6.97 (m, 1H, H_{Tp}), 6.87 (t, $^3J_{HH}$ = 7.8 Hz, 1H, H_{Ph}), 6.80 (t, $^3J_{HH}$ = 7.8 Hz, 2H, H_{Ph}), 6.29 (m, 2H, H_{Tp}), 6.25 (vt, $^3J_{HH}$ = 2.0 Hz, 1H, H_{Tp}), 6.23 (d, $^3J_{HH}$ = 1.7 Hz, 1H, H_{Tp}), 6.08 (d, $^3J_{HH}$ = 7.5 Hz, 2H, H_{Ph}), 5.45 (vt, $^3J_{HH}$ = 2.0 Hz, 1H, H_{Tp}), 4.60 (d, $^2J_{HH}$ = 15.6 Hz, 1H, H_{bridge}), 4.18 (d, $^2J_{HH}$ = 16.1 Hz, 1H, H_{bridge}). ^{13}C{^{1}H} NMR (CD_2Cl_2, 125 MHz): δ 179.8 (C_{imid}Ru), 162.1 (q, $^1J_{B-C}$ = 49.9 Hz, BAr$^F_4$), 156.8 (C_{py}), 156.0 (C_{py}), 143.8 (Tp), 143.6 (Tp), 140.9 (Tp), 139.1 (C_{py}), 139.0 (C_{Ph}), 137.9 (Tp), 137.0 (Tp), 136.8 (Tp), 135.2 (BAr$^F_4$), 129.3 (q, $^2J_{C-F}$ = 31.8 Hz, BAr$^F_4$), 129.0 (C_{Ph}), 125.9 (C_{py}), 125.8 (C_{imid}), 125.2 (C_{py}), 125.1 (C_{Ph}), 125.0 (q, $^1J_{C-F}$ = 272.5 Hz, BAr$^F_4$), 123.0 (C_{Ph}), 122.9 (C_{imid}), 117.9 (BAr$^F_4$), 108.3 (Tp), 107.6 (Tp), 107.1 (Tp), 54.6(CH_2). Anal. Calcd. for $C_{112}H_{70}B_4F_{48}N_{20}Ru_2$ + 2Et_2O: C 48.02, H 3.02, N 9.33. Found: C 48.15, H 2.99, N 9.30.

*Δ,Δ-[{TpRu(κ²-C,N-3-phenyl-1-(2-picolyl)imidazol-2-ylidene)}$_2$(μ-N$_2$)][BAr$^F_4$]$_2$ (**3d**).* ^{1}H NMR (CD_2Cl_2, 500 MHz): δ 7.90 (d, $^3J_{HH}$ = 2.5 Hz, 1H, H_{Tp}), 7.82 (d, $^3J_{HH}$ = 2.9 Hz, 1H, H_{Tp}), 7.72 (br s, 9H, BAr$^F_4$ + $H_{pyridine}$), 7.65 (t, $^3J_{HH}$ = 6.2 Hz, 1H, $H_{pyridine}$), 7.55 (br s, 4H, BAr$^F_4$), 7.50 (d, $^3J_{HH}$ = 2.0 Hz, 1H, H_{Tp}), 7.43 (d, $^3J_{HH}$ = 5.8 Hz, 1H, $H_{pyridine}$), 7.26 (d, $^3J_{HH}$ = 8.8 Hz, 1H, $H_{pyridine}$), 7.11 (d, $^3J_{HH}$ = 2.0 Hz, 1H, H_{imid}), 7.07 (d, $^3J_{HH}$ = 1.9 Hz, 1H, H_{imid}), 7.05 (m, 1H, H_{Ph}), 6.86 (t, $^3J_{HH}$ = 7.8 Hz, 2H, H_{Ph}), 6.33 (d, $^3J_{HH}$ = 1.5 Hz, 1H, H_{Tp}), 6.28 (m, 1H, H_{Tp}), 6.24 (m, 2H, H_{Tp}), 6.12 (d, $^3J_{HH}$ = 7.5 Hz, 2H, H_{Ph}), 6.09 (m, 1H, H_{Tp}), 5.68 (vt, $^3J_{HH}$ = 2.5 Hz, 1H, H_{Tp}), 4.62 (d, $^2J_{HH}$ = 16.1 Hz, 1H, H_{bridge}), 4.20 (d, $^2J_{HH}$ = 16.1 Hz, 1H, H_{bridge}). ^{13}C{^{1}H} NMR (CD_2Cl_2, 125 MHz): δ 179.9 (C_{imid}Ru), 162.1 (q, $^1J_{B-C}$ = 49.9 Hz, BAr$^F_4$), 156.8 (C_{py}), 156.0 (C_{py}), 143.7 (Tp), 143.6 (Tp), 140.8 (Tp), 139.1 (C_{py}), 139.0 (C_{Ph}), 137.9 (Tp), 136.9 (Tp), 136.8 (Tp), 135.2 (BAr$^F_4$), 129.3 (q, $^2J_{C-F}$ = 31.8 Hz, BAr$^F_4$), 129.0 (C_{Ph}), 125.7 (C_{py}), 125.7 (C_{imid}), 125.3 (C_{py}), 125.1 (C_{Ph}), 125.0 (q, $^1J_{C-F}$ = 272.5 Hz, BAr$^F_4$), 122.8 (C_{Ph}), 120.9 (C_{imid}), 117.9 (BAr$^F_4$), 107.6 (Tp), 107.2 (Tp), 107.1 (Tp), 54.5 (CH_2).

*[TpRu(κ²-C,N-3-methyl-1-(2-picolyl)imidazol-2-ylidene)(CH$_3$CN)][BAr$^F_4$] (**4a**).* [TpRu(κ²-C,N-picolyl-^{Me}I)Cl] (105.5 mg, 0.2 mmol) and NaBAr$^F_4$ (177.2 mg, 0.2 mmol) were suspended in 6 mL of acetonitrile, and an orange solution was observed. The mixture was stirred for 1 h. The solvent was removed under reduced pressure. The solid was dissolved in Et_2O (10 mL) and filtered through a pad of Celite to remove NaCl. The resulting orange solution was layered with petroleum ether to yield dark yellow crystals. Yield: 256.1 mg (92%).

dx.doi.org/10.1021/ic302553z | Inorg. Chem. 2013, 52, 4396−4410

^{1}H NMR ($CDCl_3$, 400 MHz): δ 7.86 (d, $^3J_{HH}$ = 2.4 Hz, 1H, H_{Tp}), 7.80 (d, $^3J_{HH}$ = 2.5 Hz, 1H, H_{Tp}), 7.78 (d, $^3J_{HH}$ = 2.4 Hz, 1H, H_{Tp}), 7.70 (br s, 8H, BAr^F_4), 7.57 (d, $^3J_{HH}$ = 5.8 Hz, 1H, $H_{pyridine}$), 7.51 (br s, 5H, BAr^F_4 + $H_{pyridine}$), 7.45 (d, $^3J_{HH}$ = 1.5 Hz, 1H, H_{Tp}), 7.36 (d, $^3J_{HH}$ = 1.5 Hz, 1H, H_{Tp}), 7.21 (d, $^3J_{HH}$ = 7.2 Hz, 1H, $H_{pyridine}$), 7.00 (d, $^3J_{HH}$ = 2.1 Hz, 1H, H_{imid}), 6.90 (t, $^3J_{HH}$ = 6.7, 1.4 Hz, 1H, $H_{pyridine}$), 6.73 (d, $^3J_{HH}$ = 2.1 Hz, 1H, H_{imid}), 6.35 (vt, $^3J_{HH}$ = 2.2 Hz, 1H, H_{Tp}), 6.22 (vt, $^3J_{HH}$ = 2.2 Hz, 1H, H_{Tp}), 6.00 (vt, $^3J_{HH}$ = 2.3 Hz, 1H, H_{Tp}), 5.94 (d, $^3J_{HH}$ = 1.5 Hz, 1H, H_{Tp}), 5.54 (d, $^2J_{HH}$ = 15.1 Hz, 1H, H_{bridge}), 4.95 (d, J = 15.1 Hz, 1H, H_{bridge}), 2.37 (s, 3H, NCH_3), 2.20 (s, 3H, CH_3). $^{13}C\{^1H\}$ NMR ($CDCl_3$, 101 MHz): δ 189.0 (C_{imid}Ru), 161.7 (q, $^1J_{B-C}$ = 49.8 Hz, BAr^F_4), 157.8 (C_{py}), 157.1 (C_{py}), 144.0 (Tp), 142.6 (Tp), 141.5 (Tp), 136.3 (Tp), 136.2 (Tp), 136.2 (Tp), 135.6 (C_{py}), 134.8 (BAr^F_4), 128.9 (q, $^2J_{C-F}$ = 27.9 Hz, BAr^F_4), 124.5 (q, $^1J_{C-F}$ = 272.2 Hz, BAr^F_4), 123.9 (C_{py}), 123.7 (C_{py}), 122.9 (C_{imid}), 121.5 (C_{imid}), 117.5 (BAr_4^F), 106.6 (Tp), 106.6 (Tp), 106.5 (Tp), 54.8 (CH_2), 35.3 (NCH_3), 3.9 (CH_3). Anal. Calcd. for $C_{53}H_{36}B_2F_{24}N_{10}Ru$: C 45.74, H 2.61, N 10.07. Found: C 45.77, H 2.56, N 9.99.

*[TpRu(κ^2-C,N-3-isopropyl-1-(2-picolyl)imidazol-2-ylidene)(η^2-CH_2=CH_2)][BAr^F_4] (**5b**).* [TpRu(κ^2-C,N-picolyl-^{iPr}I)Cl] (110.2 mg, 0.2 mmol) and $NaBAr^F_4$ (177.2 mg, 0.2 mmol) were suspended in 6 mL of fluorobenzene under 1 atm of ethylene, and a dark yellow solution was observed. The mixture was stirred for 1 h. The solvent was removed under reduced pressure. The solid was dissolved in Et_2O (10 mL) and filtered through a pad of Celite to remove NaCl. The resulting yellow solution was layered with petroleum ether to yield yellow crystals. Yield: 272.8 mg (97%). ^{1}H NMR (CD_2Cl_2, 400 MHz): δ 7.97 (d, $^3J_{HH}$ = 2.0 Hz, 1H, H_{Tp}), 7.87 (d, $^3J_{HH}$ = 2.4 Hz, 1H, H_{Tp}), 7.82 (d, $^3J_{HH}$ = 2.4 Hz, 1H, H_{Tp}), 7.77 (d, $^3J_{HH}$ = 2.0 Hz, 1H, H_{Tp}), 7.71 (br s, 9H, BAr^F_4 + H_{Tp}), 7.69 (t, $^3J_{HH}$ = 7.8 Hz, 1H, $H_{pyridine}$), 7.64 (d, $^3J_{HH}$ = 5.9 Hz, 1H, $H_{pyridine}$), 7.55 (br s, 4H, BAr^F_4), 7.31 (d, $^3J_{HH}$ = 6.7 Hz, 1H, $H_{pyridine}$), 7.22 (d, $^3J_{HH}$ = 2.0 Hz, 1H, H_{imid}), 7.06 (d, $^3J_{HH}$ = 2.3 Hz, 1H, H_{imid}), 6.97 (t, $^3J_{HH}$ = 6.5 Hz, 1H, $H_{pyridine}$), 6.46 (vt, $^3J_{HH}$ = 2.2 Hz, 1H, H_{Tp}), 6.28 (vt, $^3J_{HH}$ = 2.2 Hz, 1H, H_{Tp}), 6.07 (vt, $^3J_{HH}$ = 2.4 Hz, 1H, H_{Tp}), 5.83 (d, $^3J_{HH}$ = 2.0 Hz, 1H, H_{Tp}), 4.91 (d, $^2J_{HH}$ = 16.1 Hz, 1H, H_{bridge}), 4.71 (d, $^2J_{HH}$ = 16.1 Hz, 1H, H_{bridge}), 4.02 (m, 2H, CH_2), 3.71 (m, 2H, CH_2), 2.79 (m, $^3J_{HH}$ = 6.6 Hz, 1H, NC*H*), 1.09 (d, $^3J_{HH}$ = 6.8 Hz, 3H, CH_3), 0.60 (d, $^3J_{HH}$ = 6.4 Hz, 3H, CH_3). $^{13}C\{^1H\}$ NMR (CD_2Cl_2, 100 MHz): δ 180.9 (C_{imid}Ru), 162.1 (q, $^1J_{B-C}$ = 49.6 Hz, BAr^F_4), 157.3 (C_{py}), 156.9 (C_{py}), 146.0 (Tp), 144.5 (Tp), 143.2 (Tp), 138.3 (C_{py}), 138.1 (Tp), 136.6 (Tp), 136.2 (Tp), 135.2 (BAr^F_4), 129.3 (q, $^2J_{C-F}$ = 35.3 Hz, BAr^F_4), 125.1 (C_{py}), 125.0 (q, $^1J_{C-F}$ = 272.4 Hz, BAr^F_4), 124.6 (C_{py}), 123.8 (C_{imid}), 118.7 (C_{imid}), 117.9 (BAr^F_4), 107.5 (Tp), 107.1 (Tp), 106.8 (Tp), 70.8 (CH_2), 53.6 (CH_2), 50.5 (NCH), 25.4 (CH_3), 22.7 (CH_3). Anal. Calcd. for $C_{55}H_{41}B_2F_{24}N_9Ru$: C 46.96, H 2.94, N 8.96. Found: C 47.04, H 2.88, N 9.03.

*[{TpRu(κ^2-C,N-3-methyl-1-(2-picolyl)imidazol-2-ylidene)}$_2$(μ-S_2)][BAr^F_4]$_2$ (**6**).* [TpRu(κ^2-C,N-picolyl-^{Me}I)Cl] (105.5 mg, 0.2 mmol), $NaBAr^F_4$ (177.2 mg, 0.2 mmol), and an excess of sulfur (ca. 4 equiv) were suspended in 6 mL of fluorobenzene, and a dark yellow solution was observed. The mixture was stirred for 1 h. The solvent was removed under reduced pressure. The solid was dissolved in Et_2O (10 mL) and filtered through a pad of Celite to remove NaCl. The resulting orange solution was layered with petroleum ether to yield yellow crystals. Yield: 492.4 mg (89%). ^{1}H NMR (CD_2Cl_2, 400 MHz): δ 8.07 (m, 2H, H_{Tp}), 7.88 (m, 2H, H_{Tp}), 7.86 (dd, $^3J_{HH}$ = 2.5, 0.7 Hz, 1H, H_{Tp}), 7.84 (dd, $^3J_{HH}$ = 2.3, 0.7 Hz, 1H, H_{Tp}), 7.71 (br s, 18H, BAr^F_4 + $H_{pyridine}$), 7.53 (br s, 10H, BAr^F_4 + $H_{pyridine}$), 7.27 (vt, $^3J_{HH}$ = 2.1 Hz, 2H, H_{imid}), 6.91 (m, 2H, $H_{pyridine}$), 6.87 (d, $^3J_{HH}$ = 5.9 Hz, 1H, $H_{pyridine}$), 6.83 (d, $^3J_{HH}$ = 5.7 Hz, 1H, $H_{pyridine}$), 6.83 (d, $^3J_{HH}$ = 2.1 Hz, 2H, H_{imid}), 6.60 (d, $^3J_{HH}$ = 1.6 Hz, 1H, H_{Tp}), 6.56 (d, $^3J_{HH}$ = 1.4 Hz, 1H, H_{Tp}), 6.51 (d, $^3J_{HH}$ = 1.6 Hz, 1H, H_{Tp}), 6.45 (d, $^3J_{HH}$ = 1.4 Hz, 1H, H_{Tp}), 6.31 (m, 4H, H_{Tp} + H_{bridge}), 6.19 (m, 2H, H_{Tp}), 6.15 (m, 2H, H_{Tp}), 6.09 (vt, $^3J_{HH}$ = 2.1 Hz, 1H, H_{Tp}), 6.05 (vt, $^3J_{HH}$ = 2.1 Hz, 1H, H_{Tp}), 5.21 (d, $^2J_{HH}$ = 16.2 Hz, 1H, H_{bridge}), 5.19 (d, $^2J_{HH}$ = 16.2 Hz, 1H, H_{bridge}), 2.12 (s, 3H, NCH_3), 2.11 (s, 3H, NCH_3). $^{13}C\{^1H\}$ NMR (CD_2Cl_2, 101 MHz): δ 174.3 (C_{imid}Ru), 174.2 (C_{imid}Ru), 162.1 (q, $^1J_{B-C}$ = 49.9 Hz, BAr^F_4), 156.4 (C_{py}), 156.4 (C_{py}), 156.1 (C_{py}), 156.0 (C_{py}), 145.2 (Tp), 145.2 (Tp), 143.3 (Tp), 143.3 (Tp), 142.7 (Tp), 142.6 (Tp), 139.5 (C_{py}), 138.5 (Tp), 137.7 (Tp), 137.6 (Tp), 136.8 (Tp), 135.2 (BAr^F_4), 129.2 (q, $^2J_{C-F}$ = 31.5 Hz, BAr^F_4), 125.4 (C_{py}), 125.3 (C_{py}), 125.3 (C_{py}), 125.3 (C_{py}), 124.9 (q, $^1J_{C-F}$ = 272.3 Hz, BAr^F_4), 124.4 (C_{imid}), 124.3 (C_{imid}), 123.2 (C_{imid}), 123.1 (C_{imid}), 117.9 (BAr^F_4), 109.4 (Tp), 107.2 (Tp), 107.1 (Tp), 106.9 (Tp), 55.6 (CH_2), 55.5 (CH_2), 35.7 (NCH_3). Anal. Calcd. for $C_{102}H_{66}B_4F_{48}N_{18}Ru_2S$: C 44.30, H 2.41, N 9.12. Found: C 44.39, H 2.45, N 9.16.

*Experimental Determination of K_{eq} for the Equilibrium between **3d**, **3′d**, and **3″d** and **3e**, **3′e**, and **3″e**, and Its Dependence with Temperature.* ^{1}H NMR integrals were used to calculate the percentage in solution of the species involved in the equilibrium. The equilibrium constant for the process shown in eq 2 is

$$K_{eq} = \frac{[3''d]^2}{[N_2][3d - 3'd]}$$

The concentration of N_2 in solution is assumed to be constant (equal to the solubility of N_2 in nitromethane), given the experiment was conducted under a dinitrogen atmosphere in N_2-saturated solvent. As the solution is saturated with N_2, the temperature-dependence of the solubility was not taken into account in the equilibrium constant calculation. By measuring the concentration of the species in solution at different temperatures, the corresponding values of K_{eq} can be determined. A plot of ln K_{eq} versus $1/T$ allowed the calculation of $\Delta H°$ and $\Delta S°$ for the process.

Crystal Structure Analysis. Crystals of **1b**, **2a**, **2d**, **3′a**, **3′d**, **5b**, **6**, and **1b**·0.35AgBr suitable for X-ray structural determination were mounted on glass fibers and then transferred to the cold nitrogen gas stream of a Bruker Smart APEX CCD three-circle diffractometer (T = 100 K) with a sealed-tube source and graphite-monochromated Mo Kα radiation (α = 0.710 73 Å), at the Servicio Central de Ciencia y Tecnología de la Universidad de Cádiz. Four sets of frames were recorded over a hemisphere of the reciprocal space by ω scans with $\delta(\omega)$ = 0.30 and an exposure of 10 s per frame. No significant decay was observed over the course of data collection. Intensity data were corrected for Lorentz and polarization effects and absorption corrections applied using SADABS.[54] The structures were solved by direct methods and refined on F^2 by full-matrix least-squares (SHELX97) by using all unique data.[55] All non-hydrogen atoms were refined anisotropically with hydrogen atoms included in calculated positions (riding model). Racemic twinning **3′a** was refined using TWIN and BASF instructions. For **2a**, **3′d**, and **6**, some disordered CF_3 groups in the anion were refined split in two complementary orientations using displacement parameter restraints. The program ORTEP-3 was used for plotting.[56] In the Supporting Information, Table S1 summarizes the crystal data and data collection and refinement details for **1b**, **2a**, **2d**, **3′a**, **3′d**, **5b**, **6**, and **1b**·0.35AgBr. CCDC 911352−911359 contain supplementary crystallographic data for this article. These data can be obtained free of charge on application to the CCDC, 12 Union Road, Cambridge CB2 1EZ, U.K. (Fax, +44−1223−336−033; E-mail, deposit@ccdc.cam.ac.uk) and via www.ccdc.cam.ac.uk/data_request/cif.

■ ASSOCIATED CONTENT

Ⓢ Supporting Information

Experimental procedures for the synthesis of **1c−e**, **2a−c**, **3e**, **3′e**, **3″e**, **4b**, and **5a**, CIF files and crystallographic data for compounds **1b**, **2a**, **2d**, **3′a**, **3′d**, **5b**, **6**, and **1b**·0.35AgBr, and van't Hoff plots. This material is available free of charge via the Internet at http://pubs.acs.org.

■ AUTHOR INFORMATION

Corresponding Author

*(P.V.) E-mail: pedro.valerga@uca.es.

Notes

The authors declare no competing financial interest.

■ ACKNOWLEDGMENTS

We thank the Spanish MICINN (Project CTQ2010-15390) and "Junta de Andalucía" (PAI-FQM188 and Project of Excellence P08-FQM-03538) for financial support, Johnson Matthey plc for generous loans of ruthenium trichloride, and Dr. Rodrigo Alcántara who recorded the Raman spectroscopy data included in this article. F.E.F. acknowledges the spanish MICINN for a FPI fellowship (BES-2008-006635).

■ REFERENCES

(1) (a) Mercs, L.; Albrecht, M. *Chem. Soc. Rev.* **2010**, *39*, 1903−1912. (b) Díez-González, S.; Marion, N.; Nolan, S. P. *Chem. Rev.* **2009**, *109*, 3612−3676. (c) Hahn, F. E.; Jahnke, M. C. *Angew. Chem., Int. Ed.* **2008**, *47*, 3122−3172. (d) Nolan, S. P.; Clavier, H. *Annu. Rep. Prog. Chem., Sect. B* **2007**, *103*, 193−222. (e) Nolan, S. P. *N-Heterocyclic Carbenes in Synthesis*; Wiley-VCH: New York, 2006. (f) Herrmann, W. A. *Angew. Chem., Int. Ed.* **2002**, *41*, 1290−1309. (g) Bourissou, D.; Guerret, O.; Gabbai, F. P.; Bertrand, G. *Chem. Rev.* **2000**, *100*, 39−91.

(2) Normand, A. T.; Cavell, K. J. *Eur. J. Inorg. Chem.* **2008**, 2781−2800.

(3) (a) Cabeza, J. A.; Damonte, M.; García-Álvarez, P.; Kennedy, A. R.; Pérez-Carreño, E. *Organometallics* **2011**, *30*, 826−833. (b) Hahn, F. E.; Naziruddin, A. R.; Hepp, A.; Pape, T. *Organometallics* **2010**, *29*, 5283−5288. (c) Song, G.; Li, X.; Song, Z.; Zhao, J.; Zhang, H. *Chem.—Eur. J.* **2009**, *15*, 5535−5544. (d) Lee, C.; Ke, W.; Chan, K.; Lai, C.; Hu, C.; Lee, H. *Chem.—Eur. J.* **2007**, *13*, 582−591. (e) Danopoulos, A. A.; Tsoureas, N.; Macgregor, S. A.; Smith, C. *Organometallics* **2007**, *26*, 253−263. (f) Lee, H. M.; Chiu, P. L.; Zeng, J. Y. *Inorg. Chim. Acta* **2004**, 4313−4321.

(4) (a) Warsink, S.; Chang, I.; Weigand, J. J.; Hauwert, P.; Chen, J.; Elsevier, C. J. *Organometallics* **2010**, *29*, 4555−4561. (b) Gnanamgari, D.; Sauer, E. L. O.; Schley, N. D.; Butler, C.; Incarvito, C. D.; Crabtree, R. H. *Organometallics* **2009**, *28*, 321−325.

(5) (a) Nielsen, D. J.; Cavell, K. J.; Skelton, B. W.; White, A. H. *Organometallics* **2006**, *25*, 4850−4856. (b) Herrman, W. A.; Gooben, L. J.; Spiegler, M. *J. Organomet. Chem.* **1997**, *547*, 357−366.

(6) (a) Cross, E. D.; Bierenstiel, M. *Coord. Chem. Rev.* **2011**, *255*, 574−590. (b) Fliedel, C.; Braunstein, P. *Organometallics* **2010**, *29*, 5614−5626. (c) Fliedel, C.; Sabbatini, A.; Braunstein, P. *Dalton Trans.* **2010**, 8820−8828. (d) Huynh, H. V.; Yeo, C. H.; Chew, Y. X. *Organometallics* **2010**, *29*, 1479−1486. (e) Wolf, J.; Labande, A.; Daran, J.; Poli, R. *Eur. J. Inorg. Chem.* **2007**, 5069−5079.

(7) (a) Gandolfi, C.; Heckenroth, M.; Neels, A.; Laurenczy, G.; Albrecht, M. *Organometallics* **2009**, *28*, 5112−5121. (b) Moore, L. R.; Cooks, S. M.; Anderson, M. S.; Schanz, H.; Griffin, S. T.; Rogers, R. D.; Kirk, M. C.; Shaughnessy, K. H. *Organometallics* **2006**, *25*, 5151−5158.

(8) (a) Takaki, D.; Okayama, T.; Shuto, H.; Matsumoto, S.; Yamaguchi, Y.; Matsumoto, S. *Dalton Trans.* **2011**, 1445−1447. (b) Downing, S. P.; Pogorzelec, P. J.; Danopoulos, A. A.; Cole-Hamilton, D. J. *Eur. J. Inorg. Chem.* **2009**, 1816−1824. (c) Xie, L.; Sun, H.; Hu, D.; Liu, Z.; Shen, Q.; Zhang, Y. *Polyhedron* **2009**, *28*, 2585−290. (d) Wang, B.; Wang, D.; Cui, D.; Gao, W.; Tang, T.; Chen, X.; Jing, X. *Organometallics* **2007**, *26*, 3167−3172. (e) Downing, S. P.; Conde Guadaño, S.; Pugh, D.; Danopulos, A. A.; Bellabarba, R. M.; Hanton, M.; Smith, D.; Tooze, R. P. *Organometallics* **2007**, *26*, 3762−3770. (f) Sun, H.; Hu, D.; Wang, Y.; Shen, Q.; Zhang, Y. *J. Organomet. Chem.* **2007**, *692*, 903−907. (g) Downing, S. P.; Danopoulos, A. A. *Organometallics* **2006**, *25*, 1337−1340.

(9) (a) Makino, T.; Yamasaki, R.; Azumaya, I.; Masu, H.; Saito, S. *Organometallics* **2010**, *29*, 6291−6297. (b) Amar, H. B.; Hassine, B. B.; Fischmeister, C.; Dixneuf, P. H.; Bruneau, C. *Eur. J. Inorg. Chem.* **2010**, 4752−4756. (c) Schneider, N.; Kruck, M.; Bellemin-Laponnaz, S.; Wadepohl, H.; Gade, L. H. *Eur. J. Inorg. Chem.* **2009**, 493−500. (d) Schneider, N.; Bellemin-Laponnaz, S.; Wadepohl, H.; Gade, L. H. *Eur. J. Inorg. Chem.* **2008**, 5587−5598. (e) Bellemin-Laponnaz, S.; Gade, L. H. *Coord. Chem. Rev.* **2007**, *251*, 718−725. (f) Poyatos, M.; Maisse-François, A.; Bellemin-Laponnaz, S.; Peris, E.; Gade, L. *J. Organomet. Chem.* **2006**, *691*, 2713−2720.

(10) (a) Pažický, M.; Loos, A.; Ferreira, M. J.; Serra, D.; Vinokurov, N.; Rominger, F.; Jäkel, C.; Hashmi, A. S. K.; Limbach, M. *Organometallics* **2010**, *29*, 4448−4458. (b) Binobaid, A.; Iglesias, M.; Beetstra, D. J.; Kariuki, B.; Dervisi, A.; Fallis, I. A.; Cavell, K. J. *Dalton Trans.* **2009**, 7099−7112. (c) Kaufhold, O.; Hahn, F. E.; Pape, T.; Hepp, A. *J. Organomet. Chem.* **2008**, *693*, 3435−3440. (d) Veige, A. S. *Polyhedron* **2008**, *27*, 3177−3189. (e) Pugh, D.; Boyle, A.; Danopoulos, A. A. *Dalton Trans.* **2008**, 1087−1094. (f) Baya, M.; Eguillor, B.; Esteruelas, M. A.; Oliván, M.; Oñate, E. *Organometallics* **2007**, *26*, 6556−6563. (g) Wright, J. A.; Danopoulos, A. A.; Motherwell, W. B.; Carroll, R. J.; Ellwood, S. *J. Organomet. Chem.* **2006**, *691*, 5204−5210. (h) Tulloch, A. A. D.; Danopoulos, A. A.; Kleinhez, A.; Light, M. E.; Hursthouse, M. B.; Eastham, G. *Organometallics* **2001**, *20*, 2027−2031.

(11) (a) Stylianides, N.; Danopoulos, A. A.; Tsoureas, N. *J. Organomet. Chem.* **2005**, *690*, 5948−5958. (b) Song, G.; Zhang, Y.; Li, X. *Organometallics* **2008**, *27*, 1936−1943. (c) Danopoulos, A. A.; Pugh, D.; Wright, J. A. *Angew. Chem., Int. Ed.* **2008**, *47*, 9765−9767.

(12) (a) Kascatan-Nebioglu, A.; Panzner, M. J.; Tessier, C. A.; Cannon, C. L.; Youngs, W. J. *Coord. Chem. Rev.* **2007**, *251*, 884−895. (b) Catalano, V.; Etogo, A. O. *J. Organomet. Chem.* **2005**, *690*, 6041−6050.

(13) (a) Tulloch, A. A. D.; Winston, S.; Danopuolos, A. A.; Eastham, G.; Hursthouse, M. B. *Dalton Trans.* **2003**, 699−708. (b) Tulloch, A. A. D.; Danopoulos, A. A.; Tooze, R. P.; Cafferkey, S. M.; Kleinhenz, S.; Hursthouse, M. B. *Chem. Commun.* **2000**, 1247−1248.

(14) (a) Pozo, C.; Iglesias, M.; Sánchez, F. *Organometallics* **2011**, *30*, 2180−2188. (b) Chang, W.; Chen, H.; Li, T.; Hsu, N.; Tingare, Y. S.; Li, C.; Liu, Y.; Su, C.; Li, W. *Angew. Chem., Int. Ed.* **2010**, *49*, 8161−8164. (c) Son, S. U.; Park, K. H.; Lee, Y.; Kim, B. Y.; Choi, C. H.; Lah, M. S.; Jang, Y. H.; Jang, D.; Chung, Y. K. *Inorg. Chem.* **2004**, *43*, 6896−6898.

(15) (a) Benítez Junquera, L.; Puerta, M. C.; Valerga, P. *Organometallics* **2012**, *31*, 2175−2183. (b) Wang, X.; Liu, S.; Weng, L.; Jin, G. *J. Organomet. Chem.* **2005**, *690*, 2934−2940. (c) Wang, X.; Liu, S.; Jin, G. *Organometallics* **2004**, *23*, 6002−6007.

(16) Warsink, S.; van Aubel, C. M. S.; Weigand, J. J.; Liu, S. T.; Elsevier, C. J. *Eur. J. Inorg. Chem.* **2010**, 5556−5562.

(17) (a) Trofimenko, S. *Polyhedron* **2004**, *43*, 197−203. (b) Pettinari, C.; Santini, C. In *Comprehensive Coordination Chemistry II*; McCleverty, J. A., Meyer, T. J., Eds.; Pergamon: Oxford, U.K., 2004; Vol. *1*, pp 159−210. (c) Trofimenko, S. *Chem. Rev.* **1993**, *93*, 943−980. (d) Trofimenko, S. *Prog. Inorg. Chem.* **1986**, *34*, 115. (e) Trofimenko, S. *J. Am. Chem. Soc.* **1966**, *88*, 1842−1844.

(18) (a) Beach, N. J.; Williamson, A. E.; Spivak, G. J. *J. Organomet. Chem.* **2005**, *690*, 4640−4647. (b) Brunker, T. J.; Grenn, J. C.; O'Hare, D. *Inorg. Chem.* **2003**, *42*, 4366−4381. (c) Bergman, R. G.; Cundari, T. R.; Gillespie, A. M.; Gunnoe, T. B.; Harman, W. D.; Klinckman, T. R.; Temple, M. D.; White, D. P. *Organometallics* **2003**, *22*, 2331−2337. (d) Tellers, D. M.; Bergman, R. G. *Organometallics* **2001**, *20*, 4819−4832. (e) Tellers, D. M.; Bergman, R. G. *J. Am. Chem. Soc.* **2000**, *122*, 954−955. (f) Gemel, C.; Trimmel, G.; Slugovc, C.; Kremel, S.; Mereiter, K.; Schmid, R.; Kirchner, K. *Organometallics* **1996**, *15*, 3998−4004. (g) Curtis, M. D.; Shiu, K. B.; Butler, W. M.; Huffman, J. C. *J. Am. Chem. Soc.* **1986**, *108*, 3335−3343. (h) Sharp, P. R.; Bard, A. J. *Inorg. Chem.* **1983**, *22*, 2689−2693.

(19) (a) Huang, J.; Schanz, H.; Stevens, E. D.; Nolan, S. P. *Organometallics* **1999**, *18*, 2370−2375. (b) Gemel, C.; Huffman, J. C.; Caulton, K. G.; Mauthner, K.; Kirchner, K. *J. Organomet. Chem.* **2000**, *593*−*594*, 342−353. (c) Jiménez-Tenorio, M.; Mereiter, K.; Puerta, M. C.; Valerga, P. *J. Am. Chem. Soc.* **2000**, *122*, 11230−11231. (d) Halikhedkar, A.; Jiménez-Tenorio, M.; Puerta, M. C.; Valerga, P. *Organometallics* **2002**, *21*, 628−635. (e) Jiménez-Tenorio, M.; Puerta, M. C.; Valerga, P. *Eur. J. Inorg. Chem.* **2004**, 17−32. (f) Bosson, J.; Poater, A.; Cavallo, L.; Nolan, S. P. *J. Am. Chem. Soc.* **2010**, *132*, 13146−13149.

(20) Huang, J.; Stevens, E. D.; Nolan, S. P.; Petersen, J. L. *J. Am. Chem. Soc.* **1999**, *121*, 2674−2678.
(21) Huang, J.; Jafarpour, L.; Hillier, A. C.; Stevens, E. D.; Nolan, S. P. *Organometallics* **2001**, *20*, 2878−2882.
(22) (a) Baratta, W.; Herrmann, W. A.; Rigo, P.; Scharwz, J. *J. Organomet. Chem.* **2000**, *593*−*594*, 489−493. (b) Baratta, W.; Herdweck, E.; Herrmann, W. A.; Rigo, P.; Schawrz, J. *Organometallics* **2002**, *21*, 2101−2106.
(23) Pontes da Costa, A.; Mata, J. A.; Royo, B.; Peris, E. *Organometallics* **2010**, *29*, 1832−1838.
(24) Fernández, F. E.; Puerta, M. C.; Valerga, P. *Organometallics* **2011**, *30*, 5793−5802.
(25) Sandford, M. S.; Love, J. A.; Grubbs, R. H. *Organometallics* **2001**, *20*, 4314−5318.
(26) Burtscher, D.; Perner, B.; Mereiter, K.; Slugovc, C. *J. Organomet. Chem.* **2006**, *691*, 5423−5430.
(27) (a) Singh, V. K.; Bustelo, E.; de los Ríos, I.; Macías-Arce, I.; Puerta, M. C.; Valerga, P.; Ortuño, M. A.; Ujaque, G.; Lledós, A. *Organometallics* **2011**, *30*, 4014−4031. (b) de los Ríos, I.; Bustelo, E.; Puerta, M. C.; Valerga, P. *Organometallics* **2010**, *29*, 1740−179. (c) Jiménez-Tenorio, M.; Palacios, M. D.; Puerta, M. C.; Valerga, P. *J. Mol. Catal. Chem.* **2007**, *261*, 64−72. (d) Jiménez-Tenorio, M.; Palacios, M. D.; Puerta, M. C.; Valerga, P. *Organometallics* **2005**, *24*, 3088−3098. (e) Jiménez-Tenorio, M. A.; Jiménez-Tenorio, M.; Puerta, M. C.; Valerga, P. *Organometallics* **2000**, *19*, 1333−1342. (f) Jiménez-Tenorio, M. A.; Jiménez-Tenorio, M.; Puerta, M. C.; Valerga, P. *Organometallics* **1997**, *16*, 5528−5535.
(28) Pavlik, S.; Kirchner, K.; Mereiter, K. Deposition number CCDC-655657; CCDC: Cambridge, U.K., 2007.
(29) Fernández, F. E.; Puerta, M. C.; Valerga, P. *Organometallics* **2012**, *31*, 6868−6879.
(30) (a) Pavlik, S.; Schmid, R.; Kirchner, K.; Mereiter, K. *Monatsh. Chem.* **2004**, *135*, 1349−1357. (b) Standfest-Hauser, C. M.; Mereiter, K.; Schmid, R.; Kirchner, K. *Organometallics* **2004**, *23*, 2194−2196. (c) Ruba, E.; Simanko, W.; Mereiter, K.; Schmid, R.; Kirchner, K. *Inorg. Chem.* **2000**, *39*, 382−384. (d) Slugvoc, C.; Schmid, R.; Kirchner, K. *Coord. Chem. Rev.* **1999**, *185*−*186*, 109−126.
(31) (a) Mata, J. A.; Poyatos, M.; Peris, E. *Coord. Chem. Rev.* **2007**, *251*, 841−859. (b) Cheng, Y.; Xu, H.; Sun, J.; Li, Y.; Chen, X.; Xue, Z. *Dalton Trans.* **2009**, 7132−7140. (c) Zeng, F.; Yu, Z. *Organometallics* **2008**, *27*, 6025−6028. (d) Danopoulos, A. A.; Winston, S.; Motherwell, W. B. *Chem. Commun.* **2002**, 1376−1377.
(32) Jiménez-Tenorio, M.; Puerta, M. C.; Valerga, P. *Inorg. Chem.* **2010**, *49*, 6035−6057.
(33) (a) Cambridge Crystallographic Data Center. *Mogul: Retrieval of Crystallographically-Derived Molecular Geometry Information from CSD*, version 1.4 (Build RC5); CCDC: Cambridge, U.K., 2011 (b) Bruno, I. J.; Cole, J. C.; Kessler, M.; Luo, J.; Motherwell, W. D. S.; Purkis, L. H.; Smith, B. R.; Taylor, R.; Cooper, I.; Harris, S. E.; Orpen, A. G. *J. Chem. Inf. Comput. Sci.* **2004**, *44*, 2133−2144.
(34) Bennet, M. A.; Byrnes, M. J.; Chung, G.; Edwards, A. J.; Willis, A. C. *Inorg. Chim. Acta* **2005**, *358*, 1692−1708.
(35) Chatt, J.; Nokolsky, A. B.; Richards, R. L.; Sanders, J. R. *Chem. Commun.* **1969**, 154.
(36) Creutz, C.; Taube, H. *Inorg. Chem.* **1971**, *10*, 2664−2667.
(37) Jolly, P. W.; Jonas, K.; Krüger, C.; Tsay, Y. H. *J. Organomet. Chem.* **1971**, *33*, 109−122.
(38) Coia, G. M.; Demadis, K. D.; Meyer, T. J. *Inorg. Chem.* **2000**, *39*, 2212−2223.
(39) (a) Jiménez-Tenorio, M. A.; Jiménez-Tenorio, M. J.; Puerta, M. C.; Valerga, P. *J. Chem. Soc., Dalton Trans.* **1998**, 3601−3608. (b) Jiménez-Tenorio, M. A.; Jiménez-Tenorio, M. J.; Puerta, M. C.; Valerga, P. *Inorg. Chim. Acta* **1997**, *259*, 77−80.
(40) (a) Joslin, E. E.; McMullin, C. L.; Gunnoe, T. B.; Cundari, T. R.; Sabat, M.; Myers, W. H. *Organometallics* **2012**, *31*, 6851−6860. (b) Foley, N. A.; Lail, M.; Lee, J. P.; Gunnoe, T. B.; Cundari, T. T.; Petersen, J. L. *Organometallics* **2007**, *26*, 5507−5516. (c) Foley, N. A.; Lail, M.; Lee, J. P.; Gunnoe, T. B.; Cundari, T. T.; Petersen, J. L. *J. Am. Chem. Soc.* **2007**, *129*, 6765−6781.
(41) (a) Borguet, Y.; Sauvage, X.; Zaragoza, G.; Demonceau, A.; Delaude, L. *Organometallics* **2011**, *30*, 2730−2738. (b) Sauvage, X.; Borguet, Y.; Demonceau, A.; Delaude, L. *Macromol. Symp.* **2010**, *293*, 24−27. (c) Borguet, Y.; Sauvage, X.; Zaragoza, G.; Demonceau, A.; Delaude, L. *Adv. Synth. Catal.* **2009**, *351*, 441−455.
(42) (a) Wolf, J.; Thommes, K.; Brief, O.; Scopelliti, R.; Severin, K. *Organometallics* **2008**, *27*, 4464−4474. (b) Quebatte, L.; Solari, E.; Scopelliti, R.; Severin, K. *Organometallics* **2005**, *24*, 1404−1406.
(43) Miranda-Soto, V.; Grotjahn, D. B.; Cooksy, A. L.; Golen, J. A.; Moore, C. E.; Rheingold, A. L. *Angew. Chem., Int. Ed.* **2011**, *50*, 631−635.
(44) (a) Jiménez-Tenorio, M.; Palacios, M. D.; Puerta, M. C.; Valerga, P. *Organometallics* **2004**, *23*, 504−510. (b) de los Ríos, I.; Jiménez-Tenorio, M.; Padilla, J.; Puerta, M. V.; Valerga, P. *Organometallics* **1996**, *15*, 4565−4674. (c) Lindner, F.; Haustein, M.; Fawzi, R.; Steinmann, M.; Wegner, P. *Organometallics* **1994**, *13*, 5021−5029.
(45) (a) Ruba, E.; Gemel, C.; Slugovc, C.; Mereiter, K.; Schmid, R.; Kirchner, K. *Organometallics* **1999**, *18*, 2275−2280. (b) Slugovc, C.; Mauthner, K.; Kacetl, M.; Mereiter, K.; Schmid, R.; Kirchner, K. *Chem.—Eur. J.* **1998**, *4*, 2043−2050.
(46) (a) Coto, A.; de los Ríos, I.; Jiménez-Tenorio, M.; Puerta, M. C.; Valerga, P. *J. Chem. Soc., Dalton. Trans.* **1999**, 4309−4314. (b) Coto, A.; Jiménez-Tenorio, M.; Puerta, M. C.; Valerga, P. *Organometallics* **1998**, *17*, 4392−4399.
(47) Amarasekara, J.; Rauchfuss, T. B.; Wilson, S. R. *Inorg. Chem.* **1987**, *26*, 3328−3332.
(48) (a) Cornell, C. N.; Sigman, M. S. In *Activation of Small Molecule*; Tolman, W. B., Ed.; Wiley-VCH: Weinheim, Germany, 2006; pp 159−186. (b) Punniyamurthy, T.; Velusamy, S.; Iqbal, J. *Chem. Rev.* **2005**, *105*, 2329−2364. (c) Klotz, I. M.; Kurtz, D. M. *Chem. Rev.* **1994**, *94*, 567−568.
(49) Häller, L. J. L.; Mas-Marzá, E.; Moreno, A.; Lowe, J. P.; Macgregor, S. A.; Mahon, M. F.; Pregosin, P. S.; Whittlesey, M. K. *J. Am. Chem. Soc.* **2009**, *131*, 9618−9619.
(50) McGuinness, D. S.; Cavell, K. J. *Organometallics* **2000**, *19*, 741−748.
(51) Gruendemann, S.; Kovacevic, A.; Albrecht, M.; Faller, J. W.; Crabtree, R. H. *J. Am. Chem. Soc.* **2002**, *124*, 10473−10481.
(52) Tulloch, A. A. D.; Danopoulos, A. A.; Winston, S.; Kleinhenz, S.; Eastham, G. *J. Chem. Soc., Dalton Trans.* **2000**, 4499−4506.
(53) Bahr, S. R.; Boudjouk, P. *J. Org. Chem.* **1992**, *57*, 5545−5547.
(54) Sheldrick, G. M. *SADABS*, 2001 version; University of Göttingen: Göttingen, Germany, 2001.
(55) (a) Sheldrick, G. M. *SHELXTL*, version 6.10, Crystal Structure Analysis Package; Bruker AXS: Madison, WI, 2000. (b) Sheldrick, G. M. *Acta Crystallogr.* **2008**, *A64*, 112−122.
(56) Farrugia, L. J. *J. Appl. Crystallogr.* **1997**, *30*, 565.